



**HAL**  
open science

## Spatial patterning of Middle Palaeolithic lithic assemblages at the Abri du Maras, Southeast France: combining GIS analysis and 3D palaeotopographic reconstructions

Pierre Guillemot, Stéphane Jaillet, M Gema Chacón, Véronique Pois, Marie-Hélène Moncel

### ► To cite this version:

Pierre Guillemot, Stéphane Jaillet, M Gema Chacón, Véronique Pois, Marie-Hélène Moncel. Spatial patterning of Middle Palaeolithic lithic assemblages at the Abri du Maras, Southeast France: combining GIS analysis and 3D palaeotopographic reconstructions. *Journal of Archaeological Science: Reports*, 2023, 49, pp.103999. 10.1016/j.jasrep.2023.103999 . hal-04070818

**HAL Id: hal-04070818**

**<https://hal.science/hal-04070818>**

Submitted on 16 Apr 2023

**HAL** is a multi-disciplinary open access archive for the deposit and dissemination of scientific research documents, whether they are published or not. The documents may come from teaching and research institutions in France or abroad, or from public or private research centers.

L'archive ouverte pluridisciplinaire **HAL**, est destinée au dépôt et à la diffusion de documents scientifiques de niveau recherche, publiés ou non, émanant des établissements d'enseignement et de recherche français ou étrangers, des laboratoires publics ou privés.



Distributed under a Creative Commons Attribution - NonCommercial - NoDerivatives 4.0 International License

1 **Authors:**

2  
3 Pierre GUILLEMOT<sup>a\*</sup>, Stéphane JAILLET<sup>b</sup>, M. Gema CHACÓN<sup>c,d,a</sup>, Véronique POIS<sup>e</sup>  
4 Marie-Hélène MONCEL<sup>a</sup>

5  
6 <sup>a</sup> UMR 7194, CNRS, Département Homme & Environnement, Muséum National d'Histoire Naturelle, UPVD,  
7 Sorbonne Universités, 1 René Panhard, 75013, Paris, France (\* Corresponding author: [p.guillemot@icloud.com](mailto:p.guillemot@icloud.com))

8 <sup>b</sup> Laboratoire Environnement Dynamiques et Territoires de Montagne (EDYTEM), UMR 5204, 73376 Le  
9 Bourget du Lac, France.

10 <sup>c</sup> Institut Català de Paleoecologia Humana i Evolució Social (IPHES – CERCA), Zona Educativa 4, Campus  
11 Sescelades URV (Edifici W3), Tarragona 43007, Spain

12 <sup>d</sup> Departament d'Història i Història de l'Art, Universitat Rovira i Virgili (URV), Av. Catalunya 35, 43002  
13 Tarragona, Spain

14 <sup>e</sup> Université de Perpignan Via Domitia (UPVD), UMR 7194 CNRS, MNHN– HNHP, Centre Européen de  
15 Recherches Préhistoriques de Tautavel, 66720 Tautavel, France

16  
17 **Title:**

18  
19 **Spatial patterning of Middle Palaeolithic lithic assemblages at the Abri du**  
20 **Maras, Southeast France: combining GIS analysis and 3D**  
21 **palaeotopographic reconstructions**

22  
23  
24 **Abstract:**

25  
26 The intra-site spatial analysis of prehistoric assemblages is a topical way of assessing the use  
27 of space by ancient hominins. Such approaches can bring to light how prehistoric groups  
28 occupied their living space and organised activity areas, and thus describe their cultural and  
29 social behaviours. The Abri du Maras in Southeast France is a major Middle Palaeolithic site  
30 with huge potential for characterising the cognitive and technological behaviours of  
31 Neanderthals. In this study, we carry out a high-resolution spatial analysis focusing primarily  
32 on the lithic assemblages of levels 4.1 and 4.2, dated to MIS 3. The methodology combines  
33 two approaches: the use of GIS tools selected from free and open-source QGIS software, and  
34 palaeosurface rendering, using 3D software, in order to incorporate palaeotopographic data  
35 into the spatial analysis. Data for these palimpsests show a structured spatial patterning of  
36 occupations with some differences between the two levels. In level 4.1, a clear spatial pattern  
37 is observed with main areas where intense knapping activities were carried out and peripheral  
38 areas where specific remains were located. The spatial pattern for level 4.2 appears less clear,  
39 but also revealed patterns related to the type of remains. Our analysis provides evidence of  
40 complex spatial organisation for Neanderthals and corroborates previous results from other  
41 Middle Palaeolithic sites. We also highlight the relevance of our methodology, combining  
42 free and open-source GIS tools and palaeotopographic rendering, as well as the  
43 complementarity of 2D-3D tools, to achieve high-resolution spatial analysis of Palaeolithic  
44 sites.

45  
46 **Keywords:** Spatial pattern, GIS analysis, Lithic assemblages, 3D palaeotopographic  
47 rendering, Middle Palaeolithic, Abri du Maras

## 51 1. Introduction

52

53 Spatial analysis is an effective tool for assessing the relationship between  
54 archaeological material and hominin behaviours and revealing small- and large-scale spatial  
55 patterns. It consists of two main approaches: inter-site analysis and intra-site analysis (Coil,  
56 2016). Intra-site spatial analysis focuses on the material in individual sites through the study  
57 of site formation processes (taphonomy) and spatial patterning in order to assess social,  
58 economic or symbolic behaviours. In modern society, specific activities are related to  
59 particular areas (Alperson-Afil and Hovers, 2005; Anderson and Burke, 2008). Therefore, one  
60 of the assumptions underlying intra-site spatial analysis in archaeology is that similar  
61 associations can be observed in the archaeological record. Thus, spatial analysis has been an  
62 essential tool for many decades now, allowing archaeologists to better understand the  
63 behaviour of early hominins through the way they used space.

64 Due to their apparent lack of complexity, Middle Palaeolithic spatial structures have  
65 long been debated. Initially, some authors described Neanderthal spatial patterning as less  
66 complex than that of modern humans, comparing it to carnivores, such as hyenas (Pettitt,  
67 1997), or as a simple and instinctive response to the environment (Mellars, 1996). However,  
68 these ideas have been criticised and some Lower and Middle Palaeolithic spatial structures  
69 have been considered as “modern” and similar to those described for *Homo sapiens*  
70 (Alperson-Afil, 2008; Alperson-Afil et al., 2009; Alperson-Afil and Hovers, 2005; Henry,  
71 2012; Henry et al., 2004; Neruda, 2017; Oron and Goren-Inbar, 2014; Vaquero et al., 2001;  
72 Vaquero and Pastó, 2001).

73 The question of Neanderthal modernity was recently raised at the Abri du Maras. This  
74 rock shelter has yielded the oldest evidence of cord making known to date (Hardy et al.,  
75 2020). This fibre technology requires a complex knowledge of plants and the understanding  
76 of mathematical concepts for creating and managing pairs of numbers to create a string  
77 structure. Consequently, the authors consider Neanderthals as the cognitive equals of modern  
78 humans (Hardy et al., 2020). Therefore, the potential of the Abri du Maras for characterising  
79 the behaviour and technological capacities of Neanderthal has already been proven (Hardy et  
80 al., 2020, 2013; Moncel et al., 2021, 2014). In this context, this paper presents a high-  
81 resolution spatial analysis, focusing primarily on the comparison of the lithic assemblages of  
82 levels 4.1 and 4.2, dated to MIS3 (Richard et al., 2021, 2015), and considered as short-term  
83 occupations by the technological and subsistence strategies (Moncel et al., 2021, 2014). We  
84 combine innovative GIS (Geographic Information System) tools and palaeosurface rendering  
85 using 3D software. The main objective is to examine the occupation patterns of human groups  
86 at the Abri du Maras in relation to the topographical contexts of the site (Guillemot 2021).  
87 Through the study of two archaeological levels, we analyse and compare how occupants  
88 structured their inhabited space in a limited period of time.

89

## 90 2. The dataset

### 91 2.1. Chronological and archaeological context of the Abri du Maras

92

93 The Abri du Maras is a vast rock shelter located in a small valley near the Ardèche  
94 River, downstream of the Ardèche gorges. It is currently 12 m long, and 3 m deep with a  
95 ceiling height of 2 m (Combiér, 1967). The first excavations in the 1950s-1960s by R. Gilles  
96 and J. Combiér unearthed a stratigraphic sequence of eight archaeological layers with Middle  
97 Palaeolithic deposits and a Levallois laminar debitage at the top of the sequence (Moncel et  
98 al., 1994). Those layers record the gradual collapse of the cave roof over time (Debard, 1988).

99 New excavations in front of the shelter since 2006 have focused on the middle and lower part  
100 of the stratigraphic sequence, only intermittently excavated during former fieldwork.

101 The new sequence records six stratigraphic units. Stratigraphic layer 6 is currently the  
102 oldest known unit bearing evidence of human presence (Moncel et al., 2018) and lies directly  
103 on the limestone substratum (Moncel et al., 2021). Layer 5 is made up of an organic brown  
104 unit with a sandy-silty matrix (Moncel et al., 2014). Three occupation phases have been  
105 identified in this layer and dated to the end of MIS 5 (Marín et al., 2020; Richard et al., 2015).  
106 The overlying upper deposit is layer 4, 0.5 to 1 m thick, consisting of blocks of various sizes  
107 in loessic lenses. This coarse infilling contains two phases of occupation (levels 4.1 and 4.2)  
108 separated by a sterile loessic layer, dated to MIS 3 (level 4.1: between  $40 \pm 3$  ka and  $46 \pm 3$  ka  
109 ; level 4.2: between  $42 \pm 3$  ka and  $55 \pm 2$  ka) (Richard et al., 2015). More recent  
110 chronological data confirm these ages and the attribution of the sequence to MIS 3 (Richard et  
111 al., 2021). Layer 4 was deposited during progressively colder and drier conditions (Puaud et  
112 al., 2015) and the faunal corpus is composed in order of abundance of *Rangifer tarandus*,  
113 *Equus ferus* cf. *germanicus*, *Cervus elaphus*, *Bison priscus*, *Capra ibex*, *Equus hydruntinus*  
114 and *Megaloceros giganteus* (Daujeard et al., 2019). While the reindeer largely dominates the  
115 level 4.1 faunal assemblage, level 4.2 does not show such a mono-specific spectrum. Core  
116 technology consists of diverse, often short debitage sequences, including Levallois type  
117 debitage, made on local flint collected within 15-30 km of the site. The lithic assemblage and  
118 refits attest to short-term occupations with mostly unretouched flint flakes, blades, bladelets  
119 and points. Large ready-to-use flakes, blades and points were also brought to the shelter while  
120 additional *in situ* debitage produced small flakes (Moncel et al., 2021, 2014). The two layers  
121 have been considered as evidence of repeated short-term occupations.

122 The new excavations extend over a surface of around 50 m<sup>2</sup> for levels 4.1 and 4.2,  
123 which only represents part of the available surface of the shelter during human occupations.  
124 The accumulation and position of blocks from the collapse of the shelter indicate possibly the  
125 limits of the shelter ceiling during the occupation of levels 4.1 and 4.2. The ceiling border was  
126 estimated to be located in bands 8/9.

127 Excavations were conducted using a square metre grid. Each object, larger than 2 cm  
128 for faunal remains and 1 cm for lithic remains, was georeferenced in three dimensions using  
129 X, Y, and Z coordinates and recorded in a GIS database with (vertical and horizontal) spatial  
130 distribution data (Moncel et al., 2021).

131

## 132 2.2. Taphonomy and site formation processes

133

134 The study of site formation processes is an essential step in deciphering the spatial  
135 analysis of Palaeolithic sites. Taphonomy has become crucial for distinguishing natural from  
136 anthropogenic accumulation processes (Dibble et al., 1997), and assessing how intact  
137 assemblages actually are (Henry et al., 2004). As Romagnoli and Vaquero (2016) point out,  
138 determining assemblage integrity is a prerequisite for assessing human behaviours through  
139 spatial pattern analysis.

140 At the Abri du Maras, taphonomy has been investigated in several studies. Both levels  
141 have been described as a well-preserved and almost exclusive anthropogenic accumulation,  
142 showing a near absence of animal-induced modification on remains such as digested marks or  
143 carnivore and rodent tooth marks (Daujeard et al., 2019; Moncel et al., 2015; Vettese et al.,  
144 2022). From a spatial point of view, the evidence of bones in anatomical connections, the  
145 lithic and bone refits associated with short-distance connection lines, the absence of  
146 significant orientation of material, as well as the scarcity of trampling evidence suggest no  
147 major disturbance of archaeological remains (Daujeard et al., 2019; Moncel et al., 2021, 2014;

148 Vignes, 2021) allowing us to conclude that the artefacts have not undergone any major spatial  
 149 (horizontal or vertical) displacement (Moncel et al., 2015).

150 However, one particular part of the site shows post-depositional disturbances that have  
 151 been identified during fieldwork. Beyond bands 8/9 in the southeast part of the shelter, the site  
 152 is partially eroded due to the collapse of the shelter and the development of a small valley in  
 153 front of the site. The material in this sector encountered some disturbances and will not be  
 154 taken into account for this work.

155  
 156

### 157 2.3. Spatial database

158

159 The lithic database, grouping all the coordinated lithic remains and their characteristics  
 160 (length, width, type of rock, typological determination) was intensively exploited for the GIS  
 161 spatial analysis of the lithic assemblages. We also used spatial information on charcoal  
 162 remains and bone remains. As our research focuses on lithic assemblages, no detailed spatial  
 163 analysis of bones was undertaken. We merely visualised the general scattering of bones and  
 164 compared them to the more detailed spatial analysis of the lithic material. We also used data  
 165 from lithic refits; namely the analysis of lithic refits from level 4.2, as the spatial analysis of  
 166 lithic refits from level 4.1 has been published elsewhere (Moncel et al., 2021). Lithic  
 167 assemblage composition is quite similar for both levels and mainly composed of flakes and  
 168 flake fragments (including in both cases some Levallois flakes), laminar products, points and  
 169 cores (Table 1).

170

	Level 4.1	Level 4.2
Flakes (all sizes)	981	984
Flake fragments	340	243
Blades-bladelets	208	100
Points	81	55
Handaxes		1
Cores	51	38
Entire-broken pebbles	32	25
Debris	347	97
Undetermined		72
Total lithic artefacts:	2040	1615
<i>Including tools</i>	<i>50</i>	<i>81</i>
Bone remains	2734	3099
Ash lenses	7	3
Charcoal remains	127	97

171 *Table 1. Technological categories of lithic assemblages and other artefacts from levels 4.1 and 4.2*

172           2.4.3D data

173  
174           For the palaeotopographic rendering of the two archaeological levels, we used the 3D  
175 point cloud of the Abri du Maras. Laser scanning was carried out during the 2019 campaign  
176 using a 360 Light Detection And Ranging (LiDAR) terrestrial laser scanner (Faro Focus).  
177 During acquisition, 42 scans were performed. These “scenes” were then assembled, using  
178 *3DReshaper* software, into a single point cloud of 70 million points, representing the whole  
179 shelter.

180           Since the scan was carried out several years after the excavation of levels 4.1 and 4.2  
181 (excavations have currently reached layer 5), the 3D model does not show their respective  
182 topographies. Indeed, the 3D survey is carried out at a given moment of the excavation work  
183 and gives a 3D image of the surface in its state of progress during the excavation. Therefore,  
184 we used the following methodology to reconstruct them in the 3D model of the Abri du  
185 Maras.  
186

187 **3. Methods**

188  
189           3.1.3D palaeotopographic rendering

190  
191           The method of palaeotopographic rendering and analysis was carried out in three  
192 stages (Fig. 1). We began by cleaning and meshing the point cloud to obtain cleaned surface-  
193 based information (Jaillet et al., 2014), more suitable for the next steps. We also performed a  
194 rotation and three translations (in X, Y, Z coordinates) to obtain a model in the same  
195 coordinate system as the one chosen for excavations at the Abri du Maras.

196           The second stage consisted of surface rendering using the stratigraphic section  
197 drawings, which were drawn manually during past excavations and then computerised. Five  
198 section drawings were used, showing the stratigraphic limits of the two levels at different  
199 locations of the site. We proceeded as follows:

- 200           1. we created vertical planes georeferenced at the exact location of the section drawings,
- 201           2. we built texture on these planes by projecting the computerised section drawings  
202           (Previously saved as a JPEG file),
- 203           3. we digitalised points on the stratigraphic limits of the two archaeological levels shown  
204           by the projected section drawings,
- 205           4. the obtained point clouds were then meshed to obtain surface-based information  
206           representing the base of each archaeological level.

207           The final step was to analyse the 3D topographies in more detail. We chose to go back  
208 to 2D by rasterising them on CloudCompare software (using the average cell height method  
209 and a cell size of 0,008 x 0,008 m). This process transforms a 3D surface into a Digital  
210 Terrain Model (DTM), which is a digital picture where each pixel contains a value  
211 representing elevation information (ESRI, 2016). Finally, we uploaded these DTM files into  
212 QGIS software and used the “profile tool” plugin to analyse the topography (Fig. 1). Several  
213 longitudinal (west-east) and transversal (north-south) profiles were made on the DTM passing  
214 through areas of high material density identified by the spatial analysis, allowing us to study  
215 the relationship between archaeological spatial structures and the floor topography during  
216 human occupation.

221  
222  
223  
224  
225  
226  
227  
228  
229  
230  
231  
232  
233  
234  
235  
236  
237  
238  
239  
240  
241  
242  
243  
244  
245  
246  
247  
248  
249  
250  
251  
252  
253  
254  
255  
256  
257  
258  
259  
260  
261  
262  
263  
264  
265  
266  
267  
268  
269  
270

### 3.2. GIS spatial analysis

The lithic database was imported into QGIS software 3.18 version (QGIS.org, 2021). Due to the high density of artefacts, scattering maps (where each item is represented by a symbol) do not show any clear distribution patterns. We thus used the following method for more in-depth spatial patterning.

#### 3.2.1 General scattering of artefacts: average nearest neighbour

The first step is to statistically characterise the overall scattering of material. Average nearest neighbour is a method used to estimate whether the general pattern is dispersed, clustered or random (de la Torre et al., 2019; Moncel et al., 2021; Sánchez-Romero et al., 2021). If the null hypothesis is rejected, then we can apply “local methods” to identify subzones with clustering or dispersion phenomena (Sánchez-Romero et al., 2021).

#### 3.2.2 Local analysis

Two different local methods were used to ensure the reliable identification of clusters:

- (1) **Kernel density.** This is one of the most common and effective methods (Baxter et al., 1997). It converts a vectorial point layer into a raster heat map where the colour gradient depends on material density. This method calculates the density of point features around each output raster cell (the pixel size was set at 0.01 m, resulting in a low-pixel image with better resolution). A smoothly curved surface is created over each point and spreads to a specific radius around the points. Density value is highest at the point’s location and decreases with increasing distance. It reaches zero at the limit of the search radius distance (set as 0.5 m which is probably the best adapted for our data). The sum of the overlapping Kernel surfaces is then calculated for each pixel (Alperson-Afil, 2008; Alperson-Afil et al., 2009; Oron and Goren-Inbar, 2014; Stavrova et al., 2019). Finally, we standardized densities using maximum values to obtain a uniform scale (from 0 to 1), to facilitate comparisons (Alperson-Afil, 2008; Alperson-Afil et al., 2009, 2007; Coil et al., 2020). Despite the popularity of this method, criticisms of its subjective aspects have emerged (the fact that the analyst has to input a search radius) and of its lack of statistical criteria to identify clusters (Sánchez-Romero et al., 2021; Stavrova et al., 2019).
- (2) **Hotspot analysis.** Recently, statistical methods have become widely used tools for conferring statistical significance on the cluster identification process (de la Torre et al., 2019; Gabucio et al., 2023; Giusti et al., 2018; Mora Torcal et al., 2020; Reeves et al., 2019; Romagnoli and Vaquero, 2016; Sánchez-Romero et al., 2021, 2020, 2016; Spagnolo et al., 2020, 2019; Stavrova et al., 2019). Among the various methods, hotspot analysis, using the Getis-Ord  $G_i^*$  statistic (Getis and Ord, 1992; Ord and Getis, 1995), appears to be particularly effective. We used the “Hotspot Analysis” plugin, available on QGIS since 2016 (Oxoli et al., 2018, 2017, 2016). Hotspot analysis detects statistically significant clusters based on quantitative variables and the spatial relationship between artefacts. Qualitative variables must be transformed into quantitative inputs using frequency per quadrats. We created a grid of 0.25 m<sup>2</sup> quadrats and counted items within each quadrat using the tool “count points in polygon”. Hotspot analysis can then be performed. This method identifies high

271 concentration zones, called hotspots, and low concentration zones, called coldspots.  
272 The only prerequisite for this analysis is a sample of at least 30 elements. We  
273 systematically compared results with kernel density analysis to assess the proficiency  
274 of the QGIS hotspot analysis plugin.  
275

276 Using these methods, we started by visualising the general distribution of archaeological  
277 finds considering all the lithics, bones and fire-related artefacts. Regarding the latter, it is  
278 important to note that no clearly structured hearth has been brought to light at the Abri du  
279 Maras. However, studies have shown that burnt artefacts and charcoal distribution can help to  
280 identify the locations of “phantom hearths” (Alperson-Afil, 2017, 2008; Alperson-Afil et al.,  
281 2007). Moreover, charcoal clusters may indicate dispersed hearths, as fire did not alter the  
282 surrounding sediment. Ash lenses can also point to the position of hearths or areas of ash  
283 dumping and cleaning. Consequently, we analysed the spatial pattern of fire-related artefacts  
284 to locate the position of possible hearths, or at least areas of fire-related activities.

285 Secondly, we carried out analyses by sub-categories of lithic artefacts in order to identify  
286 whether specific elements showed a particular pattern compared to others or to overall  
287 distribution. Our spatial analysis focuses in particular on stone knapping and the possible  
288 identification of the location of reduction sequences. For this purpose, the spatial analysis of  
289 Raw Material Units (RMUs) is an effective tool. RMUs incorporate the lithic material from a  
290 knapping event, or a series of knapping events carried out for the reduction of a specific  
291 nodule (Bargalló et al., 2020b; Chacón et al., 2015; Moncel et al., 2014; Vaquero, 2008;  
292 Vaquero et al., 2017). We can thus differentiate pieces brought to the site already knapped  
293 (tool kits) (Bargalló et al., 2020a, 2016; Moncel et al., 2021, 2014) from those resulting from  
294 *in situ* knapping events. Fifty-two RMUs have been described for level 4.1 (Moncel et al.,  
295 2021). Fifteen are composed of pieces introduced to the site already knapped, and a dozen  
296 indicate complete or almost complete on-site knapping sequences, with items from all stages  
297 of the *chaîne opératoire*. Thus, the spatial patterns of these RMUs may indicate the location  
298 of knapping activities and may differ from those of the tool kits. Cortical flakes represent the  
299 initial phase of the reduction sequence (Courbin et al., 2020; Oron and Goren-Inbar, 2014), so  
300 they may also indicate the place of knapping areas. Lithic refits of level 4.1 have already been  
301 published (Moncel et al., 2021), so we only performed the spatial analysis of the lithic refits  
302 from level 4.2. They can provide additional information about the knapping activities carried  
303 out on site. The examination of the spatial pattern of retouched artefacts is also a critical  
304 component of our spatial analysis as tools have already shown potential to characterize  
305 activities at the Abri du Maras (Hardy et al., 2013). We also conduct a spatial analysis based  
306 on quantitative criteria, such as the length of the artefacts, to determine whether the remains  
307 were organised according to their size. In particular, the comparison of these results with the  
308 palaeotopographic data may provide taphonomic information.  
309

## 310 4. Results

311

### 312 4.1. General scattering of artefacts

313

314 Nearest neighbour analysis was carried out to characterise the overall scattering of  
315 archaeological finds in levels 4.1 and 4.2. This statistical test was applied to all remains, and  
316 shows that spatial distribution is significantly clustered (all remains from level 4.1: score  $z = -$   
317  $55.9$ ,  $p$  value  $< 0.01$ ; all remains from level 4.2: score  $z = -63.1$ ,  $p$  value  $< 0.01$ ). We also  
318 applied this test to the three main categories of artefacts separately (level 4.1: lithics: score  $z =$   
319  $-32.7$ ,  $p$  value  $< 0.01$ ; bones: score  $z = -41.7$ ,  $p$  value  $< 0.01$ ; charcoal remains: score  $z = -$



320 7.24,  $p$  value  $< 0.01$ ; level 4.2: lithics: score  $z = -34.7$ ,  $p$  value  $< 0.01$ ; bones: score  $z = -$   
321 49.9,  $p$  value  $< 0.01$ ; charcoal remains: score  $z = -8.42$ ,  $p$  value  $< 0.01$ );. In all cases, spatial  
322 scattering is statistically clustered.

#### 323 324 4.2. General patterns of lithics, bones and fire-related artefacts in level 4.1 325

326 The hotspot analysis of level 4.1 (Fig. 2) shows that lithic, bone and charcoal clusters  
327 overlap in the same areas, especially in the north-eastern part of the excavated zone, except  
328 for square I5, where no charcoal concentrations were found. Likewise, kernel density shows  
329 the same results (Fig. S1). Statistically significant clusters of charcoals appear to be closely  
330 spatially related to the densest accumulations of burnt artefacts (Fig. 2C). Charcoal and ash  
331 lenses are observed in areas with high concentrations of lithics and bones.

332 Thus, the main clusters of bones and lithics and indicators of fire activities are  
333 concentrated in the north and north-eastern part of level 4.1. Our analysis, therefore, shows  
334 that these were probably the main activity areas in level 4.1.  
335

#### 336 4.3. Spatial patterns associated with typo-technological aspects of level 4.1 337

338 RMU flint-13 ( $n=231$ ) and RMU quartz-5 ( $n=40$ ) are the largest RMUs and include  
339 artefacts from all stages of the on-site *chaîne opératoire*. They are located in the previously  
340 identified main accumulation areas (Fig. 3), where most of the lithics, bones and charcoals are  
341 clustered. Kernel densities reveal the same spatial distributions (Fig. S2).

342 Eight out of the 10 RMUs with evidence of on-site *chaîne opératoires* show  
343 preferential concentrations in the same areas (square I5-I6 and the north-eastern part of band  
344 6). These patterns may indicate that the main knapping areas were the northern and north-  
345 eastern parts of the site. For the other two RMUs, cluster distribution (Fig. S3 and S4) appears  
346 to indicate secondary knapping areas in the western and south-western parts of the site.

347 Fifteen RMUs, made up of 26 pieces, contain artefacts brought to the site already  
348 knapped (tool kits). Only kernel density analysis can be performed because they incorporate  
349 less than 30 pieces. Their spatial distributions indicate a more random pattern than the  
350 previous RMUs (Fig. 4). They seem to be scattered over the whole site without preferential  
351 accumulation areas. This confirms that spatial patterns differ for items from *in situ* knapping  
352 events and pieces introduced to the site already knapped.

353 Cortical flakes are clustered in the main accumulation areas confirming that knapping  
354 activities probably took place in this part of the site (Fig. 5). Kernel density shows the same  
355 results (Fig. S5).

356 Figure 6 shows that lithic tools are found in square I5 and also a little in M6, areas  
357 already identified for their cluster of lithics. However, the rest of the lithic tool spatial analysis  
358 displays a different pattern to those previously highlighted, which is confirmed by kernel  
359 density (Fig. S6). A significant cluster of tools is located in the middle of the excavated area,  
360 where no other cluster has been found. Very few retouched artefacts are found in the north-  
361 eastern part, where most lithics, bones and charcoals are located.

362 Several statistically significant clusters of large and small pieces were detected (Fig.  
363 7). In the northwest, a cluster of large pieces (hotspot H1) was brought to light in an area  
364 where no particular accumulation had yet been identified. The second hotspot (H2) is mainly  
365 in square J7, where part of the lithic tools is located. The last hotspot (H3) is located in the  
366 eastern part of the site, south of the largest concentration of lithic remains. Two coldspots  
367 (clusters of small pieces) were identified. The larger one is located in the main concentration  
368 of lithic artefacts. A second coldspot (C2) to the south of H3 is composed of fewer pieces.

369 The composition of the aforementioned clusters confirms length differences between hotspots  
370 and coldspots (Table S1).

371

#### 372 *4.4. General patterns of lithics, bones, and fire-related artefacts in level 4.2*

373

374 We performed the same analyses than level 4.1 to identify the main activity areas in  
375 level 4.2. The hotspot analysis of lithics, bones and charcoals displays two main cluster areas.  
376 The most extensive one is in the north-eastern part, and the second one is in the northwest of  
377 the excavated area (Fig. 8). The largest charcoal cluster is in the western part. Kernel density  
378 shows the same results as hotspot analysis (Fig. S7).

379 Burnt lithic clusters overlap with charcoal and ash lenses (Fig. 8C). Fire-related  
380 artefacts are closely spatially related and are located in the main clusters of lithics and bones.

381

#### 382 *4.5. Spatial patterns associated with typo-technological aspects of level 4.2*

383

384 We carried out a detailed spatial analysis of the upper level 4.2. Many lithics from this  
385 level have been refitted but data from RMU analysis are still being processed.

386 Hotspot analysis (Fig. 9) and kernel density (Fig. S8) show that cortical flakes are  
387 clustered in the western part of the site. No dense zone, or meaningful cluster, is visible in the  
388 northeast, among the largest concentration of lithic artefacts. As mentioned above, we did not  
389 focus on the southeast of the site (from squares K9-L9-M9-N9) as it has undergone extensive  
390 post-depositional disturbances.

391 Out of a total of 1615 lithic remains from level 4.2, 81 are retouched artefacts.  
392 Statistically significant clusters are found in the western part of the site (Figs. 10 and S9),  
393 whereas no tool clusters are visible in the eastern part of level 4.2, where the highest  
394 concentrations of lithics and bones are found. However, lithics, bones and charcoals are also  
395 clustered in the western part of the site. Lithic tools are concentrated on the margins of those  
396 clusters, rather than in them.

397 The spatial analysis of cores also shows clustering in the west of the site (Figs. 11 and  
398 S10) and no statistical concentrations in the northeast, where the most significant clusters of  
399 remains are located.

400 We performed hotspot analysis according to artefact length to shed more light on these  
401 patterns (Fig. 12). Three clusters of large pieces can be identified, two of which are in the  
402 disturbed area. The first hotspot (H1) is located in the northwest of the site, close to where  
403 cores, tools, and clusters of lithics, bones and charcoals are found. Two other hotspots (H2  
404 and H3) are in the disturbed area of the site. A significant cluster of small artefacts (coldspot  
405 C1) is located in the north-eastern part of the site, where the highest concentration of lithics  
406 and bones was already identified. This area is thus mainly composed of small pieces, and no  
407 large pieces are found in this zone. A second coldspot (C2) is in the disturbed part of the site.  
408 The composition of the clusters confirms length differences between hotspots and coldspots  
409 (Table S2).

410 Level 4.2 comprises 22 refit groups, for a total of 53 pieces, with 29 connection lines  
411 (Fig. S11, Table S3). Most of the refits are in the main accumulation areas (northeast of the  
412 site) and only two refits are in the western part of the excavated area (Fig. S11). Most of the  
413 connection lines are between 0 and 2 m and are within the normal dispersion range for on-site  
414 knapping sequences, as shown by experimental archaeology (Cziesla, 1990; Moncel et al.,  
415 2021, 2014; Vaquero et al., 2019, 2017). Four connection lines are beyond 2 m and could  
416 suggest the intentional anthropogenic displacement of some pieces during daily activities.

417

#### 4.6. *Palaeotopography of level 4.1*

The topography of the base of the surface of level 4.1 was rendered in 3D. Most of the area was successfully interpolated, bringing to light the general topography of the level. Fig. 13A shows the dip in an altitude-dependent colour scale. The 4.1 surface shows downward dips from the northwest to the southeast, probably due in part to the compression and compaction of sediment over time. The highest elevation in the northwest corner is about -2 m above level 0, and the lowest in the southeast corner is almost -3.60 m.

The DTM and the QGIS "profile tool" plugin allow us to study the topography in more detail (Fig. 13B). Several longitudinal (west-east) and transversal (north-south) profiles were made on the DTM, passing through clusters of small and large lithic artefacts previously identified. The longitudinal sections show a slight, progressively decreasing west-east dip, with a steeper slope in the western part, clearly visible on profiles BB' and CC' (at bands E, F and G). Beyond these bands, the dip is negligible or even non-existent, as shown in the eastern half of profile CC'. The difference in elevation from one end to the other is 1 m maximum. The transversal profiles (DD' and EE') show a north-south dip, steeper than the west-east dip, with a negative gradient of almost 1 m over a distance of 3 m (section DD'). However, the slope rises slightly in the middle (band 7) and falls again.

#### 4.7. *Palaeotopography of level 4.2*

In the upper level, 3D rendering was successful for most of the area, but part of the eastern trench could not be entirely interpolated. Nevertheless, this surface provides general information on the northwest to southeast dipping topography of level 4.2 (Fig. 14A).

In QGIS, profiles were made on the DTM (Fig. 14B) and deliberately run through clusters of small and large remains to detail the topography in these areas. The W-E profiles show a gradual decrease in dip from west to east, with an altitude differential of about 1 m from one end to the other. In the western part of the site, the DD' profile shows a very slight north-south dip in the first part, followed by significant steepening of the slope and subsequent stabilising. In the eastern part, the dip decreases progressively from north to south and then significantly, with an altitudinal difference of 90 cm over a distance of 4 metres (section CC'). However, the slope rises slightly and decreases significantly again towards the centre of the surface (visible on profile EE'). The southern ends of profiles CC' (from square M9) and EE' (from square L9) correspond to the beginning of the disturbed area.

## 5. Discussion

### 5.1. *Site formation processes*

Site formation processes have to be considered when performing spatial analysis. It is a prerequisite for assessing human behaviours through spatial patterns (Romagnoli and Vaquero, 2016). As previously said, many studies have shown that both levels are well-reserved anthropogenic accumulations, with a lack of post-depositional disturbances (Daujeard et al., 2019; Moncel et al., 2021, 2015, 2014; Vettese et al., 2022; Vignes, 2021).

Our analysis completes those results. The combination of spatial analysis and topographic data is a powerful tool that can help to assess site formation processes. Indeed, disturbances, such as runoff or water flow, can alter the spatial distribution of remains, causing movement and downslope displacement (Petraglia and Potts, 1994). Spatial analysis and palaeotopographic rendering of levels 4.1 and 4.2 do not show such patterns. The areas

467 with the highest artefact density are located in the northern part of the site and follow a gentle  
468 slope. In contrast, the lowest areas (south and southeast of the site) contain fewer remains and  
469 no significant clusters of material. This pattern is general across the site and for both levels,  
470 the areas of highest densities are found in the highest part of the site, east and west, while  
471 towards the south, the artefact densities are much lower. Thus, the material is not located in  
472 the more depressed areas and is not organised following the slope, which would have been  
473 observed if levels had encountered spatial disturbances caused by water for example. In  
474 addition, water flows tend to sort archaeological remains by size (Dibble et al., 1997; Gabucio  
475 et al., 2023; Petraglia and Potts, 1994; Sánchez-Romero et al., 2020) with displacements of  
476 large pieces into hollows and the removal of smaller remains from the assemblage. Both  
477 archaeological levels comprise clusters of small items that are found in the northern part of  
478 the site, areas with gentle slopes. For level 4.1, section EE' has a slight depression and the  
479 majority of the cluster of large lithic artefacts is not located in the deepest part, but at the  
480 margins of this depressed zone. Thus, we can say that, for both levels, clusters of large pieces  
481 are not in the lowest or most depressed part of the site. The proximity of the large and small  
482 artefact clusters, especially for level 4.1, also indicates the absence of significant spatial  
483 disturbance, such as water flows.

484 Another important issue and a common feature of Palaeolithic sites is the palimpsest  
485 problem (e.g., Bailey, 2007; Galanidou, 2000; Henry, 2012; Machado et al., 2019, 2013;  
486 Malinsky-Buller et al., 2011; Mallol and Hernández, 2016; Mora Torcal et al., 2020; Picin and  
487 Cascalheira, 2020; Reeves et al., 2019; Vaquero, 2008; Vaquero et al., 2012; Vaquero and  
488 Pastó, 2001). Both levels are palimpsests of several occupations (Moncel et al., 2021, 2015),  
489 meaning that Neanderthals possibly occupied the same areas repeatedly during short-term  
490 stays in the shelter. Multiple short-term occupations of the same site during a short period of  
491 time are a common characteristic of Middle Palaeolithic sites (for this specific topic see  
492 Cascalheira and Picin, 2020). In those cases, vertical plots are commonly used to decipher  
493 palimpsests (e.g., Bargalló et al., 2020, 2016; Coil et al., 2020; Mora Torcal et al., 2020;  
494 Sañudo et al., 2012; Vaquero, 2008; Vaquero and Pastó, 2001) and although this paper  
495 focuses primarily on horizontal analysis, we also visualised vertical dispersion (Guillemot  
496 2021). But it was not possible to untangle any palimpsests.

497 However, in some cases, palimpsests are not necessarily an issue. Indeed, the rapid  
498 burial of the levels at the Abri du Maras (Moncel et al., 2021), makes them “rapid-  
499 accumulation palimpsests” (Malinsky-Buller et al., 2011). According to this model, spatial  
500 patterns and anthropogenic clusters can still be observed even though these two sub-levels are  
501 palimpsests. Moreover, following the idea of Reeves et al., (2019), palimpsests should not  
502 only be viewed as a hindrance to spatial analysis but on the contrary, can be a necessary  
503 condition for identifying behaviours. Bailey and Galanidou (2009) already suggested that  
504 palimpsests, especially in caves or rock shelters, have a great potential to give information  
505 about the use of space. The fact that the same rock shelter was used many times for many  
506 short-term occasions and probably by the same groups tends to create patterns that are  
507 repeated over time. This is mainly due to the physical conditions of caves and rock shelters  
508 (walls, ceiling, interior versus exterior...) that influenced the way of using space, and the fact  
509 that palimpsests create a living space where remains of past occupations may influence  
510 subsequent occupations (Bailey and Galanidou, 2009). Thus, these characteristics probably  
511 influence the way of re-using the same space, especially if the occupations are of similar  
512 duration. Following that idea, palimpsest does not hinder patterns but creates them. However,  
513 even if palimpsest makes patterns distinguishable, we must keep in mind that the different  
514 clusters may not be contemporaneous.

515

516 5.2. *Significance of level 4.1 spatial patterns*

517  
518 The hotspot analysis of level 4.1 identified several main activity areas associated with  
519 peripheral areas (Fig. 15A). The largest clusters of lithics, bones and fire-related remains are  
520 concentrated in the north-eastern part of the site. The analysis of cortical flakes and RMUs  
521 shows that *in situ* knapping activities took place there. This is confirmed by the presence of  
522 clusters of lithic refits in this area, with connection lines within the normal dispersion range  
523 for on-site knapping sequences (Moncel et al., 2021). Metrical analysis indicates that this area  
524 includes small flakes, which are a reliable indicator of the location of knapping activities  
525 (Henry et al., 2004; Sañudo et al., 2012; Vaquero et al., 2001; Vaquero and Pastó, 2001). All  
526 the analyses point to areas dedicated to knapping activities and surrounded by some clusters  
527 of lithic tools and large lithic artefacts (Fig. 15A). Those types of remains have been  
528 described as artefacts moved from the main activity areas to the peripheries (Vaquero et al.,  
529 2001).

530 This pattern can be compared to the "drop-toss area" model observed among modern  
531 hunter-gatherers (Binford, 1983). According to Binford, knapping activities are concentrated  
532 in areas around hearths. These areas mainly contain small pieces ("drop zone"). The reason  
533 for this is that large pieces, which could potentially hinder the continuation of the activity or  
534 are required for use elsewhere, are moved to peripheral areas ("toss zone"). Level 4.1 of the  
535 Abri du Maras displays similar spatial patterns. No hearth has been identified but ash lenses,  
536 charcoal remains, burnt lithics and their spatial relationship indicate fire-related activities and  
537 perhaps the location of short-lived hearths that did not alter the surrounding sediments.  
538 Studies have already shown that fire-related artefacts can attest to 'phantom hearths'  
539 (Alperson-Afil, 2017, 2008; Alperson-Afil et al., 2007). The knapping areas in level 4.1 seem  
540 to be closely related to fire-related activities.

541 The particular case of square I5 should be mentioned. While showing evidence of a  
542 drop zone (cluster of cortical flakes, cluster of RMU showing knapping activities and  
543 presence of refits), this square also displays a cluster of tools. Length analysis is not helpful as  
544 the results do not show statistical evidence for clusters of small or large artefacts. This  
545 mixture of features may be due to palimpsests and illustrates that some parts of the site may  
546 be difficult to understand due to repeated short-term occupations. This could also explain the  
547 presence of few lithic tools in M6.

548 This paper focuses almost exclusively on lithic material and it is thus difficult to  
549 define spatial organisation in greater detail. Level 4.1 contains evidence of intense specialised  
550 reindeer butchery activities (Daujeard et al., 2019; Moncel et al., 2021), showing that all the  
551 stages of the butchery *chaîne opératoire* were carried out *in situ* (Daujeard et al., 2019;  
552 Vettese et al., 2017). A high-resolution spatial analysis of the faunal remains will be required  
553 to complete our conclusions.

554  
555 5.3. *Significance of level 4.2 spatial patterns*

556  
557 The spatial organisation of level 4.2 is different to that of level 4.1 (Fig. 15B). We  
558 identified two main accumulation areas, possibly related to the aspect of the shelter. It is  
559 important to recall that the shelter may have been slightly larger during occupations of level  
560 4.2 than level 4.1. Neanderthals could have occupied the site differently, extending activities  
561 over a larger surface. Another explanation could be the extension of level 4.2 excavations.  
562 Indeed, compared to the above level, level 4.2 was excavated over a larger area, which could  
563 generate a bias in the understanding of the site and give the impression that Neanderthals  
564 occupied the shelter over a larger surface.

565 Area 1 presents the most significant clusters of lithics and bones. Further investigation  
566 showed that this area contains mainly small artefacts. Moreover, most of the lithic refits are  
567 from this area, with most connection lines in the normal dispersion range for on-site knapping  
568 sequences (Cziesla, 1990; Moncel et al., 2021, 2014; Vaquero et al., 2019, 2017). As with the  
569 upper level, these two characteristics appear to reveal an area used for knapping activities.  
570 Area 2, located in the western part of the site, comprises smaller clusters of lithics and bones  
571 but also contains the largest cluster of charcoals. This area includes clusters of lithic tools,  
572 cores and large artefacts. With just two refits and no clusters of small remains, it is unlikely  
573 that the western part of level 4.2 was a central location of knapping activities. Both areas  
574 attest to fire-related items, even though more intense fire activities seem to have taken place  
575 in Area 2, as shown by the higher density of charcoals. Finally, squares I6 and J6 are  
576 intriguing. They are located at the boundary of Area 1, but clusters of cores, cortical flakes  
577 and lithic tools can be observed in this zone.  
578 Binford's model seems less relevant here as it would predict more fire-related artefacts and  
579 cortical flakes in Area 1, where knapping activities have been identified. Without data on  
580 RMUs, it is difficult to describe the spatial patterning of this level in more detail. However,  
581 we clearly observe the distribution of different types of artefacts in distinct areas, and these  
582 two areas attest to very different typo-technological characteristics. The absence of refits  
583 connecting them confirms the organisation of level 4.2 into two different zones, and perhaps  
584 different and unrelated phases of site occupation. Moreover, an initial spatial analysis of  
585 faunal remains has identified a different pattern between ungulate types and according to  
586 anatomical elements. While the remains of large-sized ungulates (horse, bison, megaceros), as  
587 well as cranial and post-cranial axial skeletons, seem to be more densely concentrated in Area  
588 1, the bones of medium-sized ungulates (reindeer, red deer), and the remains of the  
589 appendicular skeletons are more concentrated in Area 2 (Vignes, 2021). This may confirm the  
590 spatial organisation of level 4.2 into two distinct areas, or unrelated phases of occupation.  
591

#### 592 5.4. *The Abri du Maras in the Middle Palaeolithic cultural context*

593

594 The spatial analysis of Middle Palaeolithic sites is an integral component of debates on  
595 the complexity of Neanderthal behaviour and social organisation (e.g., Anderson and Burke,  
596 2008; Henry et al., 2004; Oron and Goren-Inbar, 2014; Pettitt, 1997; Vaquero et al., 2001;  
597 Vaquero and Pastó, 2001). For many years, no complex spatial organisation was found for  
598 Middle Palaeolithic sites (Alperson-Afil and Hovers, 2005), sometimes due to the inherent  
599 difficulties in understanding palimpsests. This has led some authors to consider that  
600 Neanderthal social organisation was less complex than that of Modern Humans (Oron and  
601 Goren-Inbar, 2014).

602 However, that idea has now come under strong criticism, and some authors view  
603 Middle Palaeolithic spatial structures as indicative of complex organisation, similar to that of  
604 *Homo sapiens*. At the Abric Romaní (Spain, levels H, I, J, K and L dated between 45 to 52  
605 ka), the spatial layout of Neanderthal activities fits the model of hearth-related assemblages,  
606 with knapping activities systematically carried out near hearths (Vaquero et al., 2001;  
607 Vaquero and Pastó, 2001). The Jordanian Tor Faraj site (floors I and II, average age of  $55.1 \pm$   
608  $5.6$  ka) is spatially organised in a complex way, with butchery areas, final lithic and food  
609 processing areas, initial lithic processing areas and bedding areas (Henry, 2012; Henry et al.,  
610 2004). At the Amud Cave site in Israel (55 to 69 ka), sub-unit B2 comprises knapping areas  
611 and specific zones for the disposal of unusable lithic materials (Alperson-Afil and Hovers,  
612 2005). In levels 2.2 and 3 of the Crimean site of Karabi Tamchin (MIS 3), a differential use of  
613 space was observed according to activities (discard areas, tool manufacturing, bone  
614 processing and tool use areas) (Anderson and Burke, 2008). Level VII of the Amalda I Cave

615 (Spain, between ca 42 600 and 44 500 uncal BP) reveals a different spatial layout in keeping  
616 with artefact type and the length of remains (Sánchez-Romero et al., 2020). The spatial  
617 organisation of the Israeli open-air site of Quneitra ( $53 \pm 5.9$  ka BP) is delimited by knapping,  
618 butchering or marrow extraction activities (Oron and Goren-Inbar, 2014).

619 Our analysis indicates that the Neanderthal groups of the Abri du Maras structured the  
620 spatial management of the shelter, with main activity areas used for intense knapping  
621 activities and associated with fire-related activities. Other areas with specific remains, such as  
622 the largest pieces or lithic tools, were located elsewhere. These behaviours are similar to those  
623 described above; the inhabited space is structured by the type of remains and probably by the  
624 type of activities. It is important to emphasise that the spatial pattern of level 4.2 is slightly  
625 different and more difficult to interpret than level 4.1, perhaps because the shelter was  
626 occupied over a larger area or because activities were different. It is important to remember  
627 that while the lithic industry is similar for both levels, the faunal assemblage of level 4.2 is  
628 more diverse (Daujeard et al., 2019) perhaps reflecting a different type of occupation. The  
629 palaeotopographic reconstructions for the two levels do not show significant differences (a  
630 decreasing slope from northwest to southeast for both levels), and the inter-level variation of  
631 the spatial organisation was probably dictated by the social organisation or cultural choices of  
632 Neanderthal groups, such as types of activities, and not by a change in soil topography. Inter-  
633 level variations have already been observed for Middle and Upper Palaeolithic sites (e.g.,  
634 Anderson and Burke, 2008; Caron-Laviolette et al., 2018; Vaquero et al., 2001). A recent  
635 study on butchery tradition indicates that different marrow extraction methods occurred  
636 between levels 4.1 and 4.2 (Vettese et al., 2022), suggesting that the shelter was used by  
637 distinct groups with their own tradition and perhaps different group compositions or structures  
638 (more or less specialized Neanderthals). This may explain the difference in the spatial pattern  
639 between levels, both groups occupied the site differently. This variation in spatial organisation  
640 between sub-levels has yet to be confirmed by further analysis, especially spatial studies of  
641 faunal remains, level 4.2 RMU analysis and high-resolution vertical spatial analysis.

642  
643

#### 644 5.5. *Methodological aspects*

645

646 We wanted to demonstrate the efficiency of a spatial analysis carried out under a free  
647 and open source GIS software. While some authors have stressed the need to use such open  
648 source software in order to ensure a healthier scientific practice (Ducke, 2012; Ince et al.,  
649 2012; Morin et al., 2012), others have shown the advantages of open source GIS software  
650 over proprietary software for archaeological research (Orengo, 2015). This is especially  
651 important in a context where GIS has become an indispensable tool for archaeologists  
652 (Brouwer Burg, 2017; Howey and Brouwer Burg, 2017; Orengo, 2015; Richards-Rissetto,  
653 2017; Whitley, 2017). So far, hotspot analyses have only been carried out using commercial  
654 software, including ArcGIS (Mora Torcal et al., 2020; Sánchez-Romero et al., 2021, 2020;  
655 Stavrova et al., 2019). Our analysis shows the relevance of performing hotspot analysis using  
656 an open source software. We systematically compared hotspot results with kernel density  
657 analysis to test the reliability of the plugin and confidently identify clusters by combining  
658 methods (Sánchez-Romero et al., 2021). Both methods gave the same results, thus, the QGIS  
659 “Hotspot Analysis” plugin appears to be an appropriate free and open source tool for studying  
660 spatial patterns.

661 Palaeotopographic reconstruction is a valuable tool to help investigate the spatial  
662 distribution of archaeological remains (Bargalló et al., 2020a; Gabucio et al., 2023; Sánchez-  
663 Romero et al., 2020). Combined with high-resolution spatial analysis, it provides detailed  
664 behavioural and taphonomic information. The 3D method used in this paper is not just a

665 digitisation of archaeological surfaces but a reconstruction of parts of the site, which no  
666 longer existed when the laser scanning of the Abri du Maras was carried out. We have used  
667 available section drawings to reconstruct ancient topographies. While this method seems  
668 efficient, we must to emphasize that the reconstructed surfaces are imperfect, as some parts  
669 could not be interpolated correctly. This was due to the limited number of useful section  
670 drawings that have been used (some being unavailable to record or to use by the quantity of  
671 blocks due to the final collapse of the shelter). That point is essential because even if the  
672 reconstructed topographies seem coherent, we would have needed more stratigraphic section  
673 drawings, spread over the whole site area, for homogeneous, complete and more precise  
674 rendering.

675 Finally, we would like to highlight the complementarity between 2D and 3D analyses.  
676 Once the palaeosurfaces had been rendered in 3D, we chose to go back to 2D by analysing  
677 them with QGIS. In our view, the possibilities of 2D-3D back and forth have not been  
678 sufficiently underlined, even though the potentialities of "GIS + 3D" have already been  
679 discussed (Dell'Unto and Landeschi, 2022). 3D technologies offer access to new types of  
680 analysis and ultimately to a better understanding of archaeological sites (Campana, 2016;  
681 Westoby et al., 2012). At the same time, the development of GIS has led to significant  
682 advances in how we visualise, process and analyse archaeological data (McCoy and  
683 Ladefoged, 2009). But when used together, 2D and 3D methods offer excellent tools for the  
684 high-resolution spatial analysis of archaeological sites and the reconstruction of the daily  
685 activities of past human groups.

686  
687

## 688 **6. Conclusion**

689

690 The primary goal of this research was to perform a high-resolution spatial analysis of  
691 the lithic assemblages of levels 4.1 and 4.2 (MIS 3) from the Abri du Maras. By combining  
692 2D analyses, using a free and open-source GIS software, and 3D palaeotopographic  
693 reconstructions we were able to provide evidence about the use of space by Neanderthals. We  
694 have to keep in mind that both levels are palimpsests. However, even if Neanderthals  
695 repeatedly occupied the shelter in a short period of time, it is still possible to identify spatial  
696 patterns.

697 Spatial management is well-defined in level 4.1, where the main areas were used for  
698 knapping and probably associated with fire activities. Specific remains, such as large pieces or  
699 lithic tools were located on the periphery of these main areas. The spatial pattern in level 4.2  
700 was somewhat different and not as clear, with two main distinct accumulation areas related to  
701 specific typo-technological composition. Those inter-level variations of spatial organisation  
702 do not appear to be dictated by a change in soil topography but probably by cultural choices,  
703 activities or different ways of occupying the shelter surface (perhaps because the shelter was  
704 larger and occupied over a larger area). Our analysis also furnishes new evidence on site  
705 formation processes and confirms that levels at the Abri du Maras were not subject to intense  
706 post-depositional disturbances. These observations point to a complex organisation at the Abri  
707 du Maras, with a structured division of space according to the types of remains and probably  
708 the types of activities. These behaviours are similar to those described in modern hunter-  
709 gatherer models and to those observed in other Middle Palaeolithic sites with complex social  
710 organisations.

711 Future analyses, currently under study, particularly of level 4.2, may provide  
712 additional information to better understand the occupational patterns of some of the last  
713 Neanderthal groups in the Rhône Valley.

714



715  
716  
717  
718  
719  
720  
721  
722  
723  
724  
725  
726  
727  
728  
729  
730  
731  
732  
733  
734  
735  
736  
737  
738  
739  
740  
741  
742  
743  
744  
745  
746  
747  
748  
749  
750  
751  
752  
753  
754  
755  
756  
757  
758  
759  
760  
761  
762  
763  
764

## **Acknowledgements**

Fieldwork was backed by the Service de l'Archéologie, Région Auvergne-Rhône-Alpes, French Ministry of Culture.

The analyses were financed by the Museum National d'Histoire naturelle, and the CERP (Tautavel, France). M.G.CH.'s research is funded by Research Group n° 2017 SGR 836 of the Catalan Government, project PID2019-103987GB-C31) of the Ministry of Science and Innovation, CERCA Programme/Generalitat de Catalunya and the "Spanish Ministry of Science and Innovation through the 'María de Maeztu' program for Units of Excellence (CEX2019-000945-M).

3D analysis was carried out at the Pôle Images 5D of the Laboratoire EDYTEM.

The English manuscript was edited by L. Byrne, an official translator and native English speaker.

We thank the editor and the reviewers for their useful comments that enriched and improved our paper.

**Declarations of interest:** none

## **References**

Alperson-Afil, N., 2017. Spatial Analysis of Fire: Archaeological Approach to Recognizing Early Fire. *Current Anthropology* 58, S258–S266. <https://doi.org/10.1086/692721>

Alperson-Afil, N., 2008. Continual fire-making by Hominins at Gesher Benot Ya'aqov, Israel. *Quaternary Science Reviews* 27, 1733–1739. <https://doi.org/10.1016/j.quascirev.2008.06.009>

Alperson-Afil, N., Hovers, E., 2005. Differential use of space at the Neandertal site of Amud Cave, Israel. *Eurasian Prehistory* 3, 3–22.

Alperson-Afil, N., Richter, D., Goren-Inbar, N., 2007. Phantom hearths and the use of fire at Gesher Benot Ya' Aqov, Israël. *PaleoAnthropology* 7, 1–15.

Alperson-Afil, N., Sharon, G., Kislev, M., Melamed, Y., Zohar, I., Ashkenazi, S., Rabinovich, R., Biton, R., Werker, E., Hartman, G., Feibel, C., Goren-Inbar, N., 2009. Spatial Organization of Hominin Activities at Gesher Benot Ya'aqov, Israel. *Science* 326, 1677–1680. <https://doi.org/10.1126/science.1180695>

Anderson, K.L., Burke, A., 2008. Refining the definition of cultural levels at Karabi Tamchin: a quantitative approach to vertical intra-site spatial analysis. *Journal of Archaeological Science* 35, 2274–2285. <https://doi.org/10.1016/j.jas.2008.02.011>

Bailey, G., 2007. Time perspectives, palimpsests and the archaeology of time. *Journal of Anthropological Archaeology* 26, 198–223. <https://doi.org/10.1016/j.jaa.2006.08.002>

Bailey, G., Galanidou, N., 2009. Caves, palimpsests and dwelling spaces: examples from the Upper Palaeolithic of south-east Europe. *World Archaeology* 41, 215–241. <https://doi.org/10.1080/00438240902843733>

765  
766 Bargalló, A., Gabucio, M.J., Gómez de Soler, B., Chacón, M.G., Vaquero, M., 2020a. A  
767 Snapshot of a Short Occupation in the Abric Romaní Rock Shelter: Archaeo-Level Oa, in:  
768 Cascalheira, J., Picin, A. (Eds.), *Short-Term Occupations in Paleolithic Archaeology,*  
769 *Interdisciplinary Contributions to Archaeology.* Springer International Publishing, Cham,  
770 pp. 217–235. [https://doi.org/10.1007/978-3-030-27403-0\\_9](https://doi.org/10.1007/978-3-030-27403-0_9)  
771  
772 Bargalló, A., Gabucio, M.J., Rivals, F., 2016. Puzzling out a palimpsest: Testing an  
773 interdisciplinary study in level O of Abric Romaní. *Quaternary International, Advances in*  
774 *Palimpsest Dissection 417*, 51–65. <https://doi.org/10.1016/j.quaint.2015.09.066>  
775  
776 Bargalló, A., Gabucio, M.J., Soler, B.G. de, Chacón, M.G., Vaquero, M., 2020b.  
777 Rebuilding the daily scenario of Neanderthal settlement. *Journal of Archaeological*  
778 *Science: Reports 29*, 102139. <https://doi.org/10.1016/j.jasrep.2019.102139>  
779  
780 Baxter, M.J., Beardah, C.C., Wright, R.V.S., 1997. Some archaeological applications of  
781 kernel density estimates. *Journal of Archaeological Science 24*, 347–354.  
782  
783 Binford, L.R., 1983. *In pursuit of the past: decoding the archaeological record.* Thames  
784 and Hudson, London.  
785  
786 Brouwer Burg, M., 2017. It must be right, GIS told me so! Questioning the infallibility of  
787 GIS as a methodological tool. *Journal of Archaeological Science 84*, 115–120.  
788 <https://doi.org/10.1016/j.jas.2017.05.010>  
789  
790 Campana, S. (Ed.), 2016. *Proceedings of the 43rd Annual Conference on Computer*  
791 *Applications and Quantitative Methods in Archaeology,* Archaeopress archaeology.  
792 Archaeopress Publishing Ltd, Oxford.  
793  
794 Caron-Laviolette, E., Bignon-Lau, O., Olive, M., 2018. (Re)occupation: Following a  
795 Magdalenian group through three successive occupations at Étioilles. *Quaternary*  
796 *International 498*, 12–29. <https://doi.org/10.1016/j.quaint.2018.10.043>  
797  
798 Cascalheira, J., Picin, A. (Eds.), 2020. *Short-Term Occupations in Paleolithic*  
799 *Archaeology: Definition and Interpretation,* *Interdisciplinary Contributions to*  
800 *Archaeology.* Springer International Publishing, Cham. [https://doi.org/10.1007/978-3-](https://doi.org/10.1007/978-3-030-27403-0)  
801 [030-27403-0](https://doi.org/10.1007/978-3-030-27403-0)  
802  
803 Chacón, M.G., Bargalló, A., Gabucio, M.J., Rivals, F., Vaquero, M., 2015. Neanderthal  
804 Behaviors from a Spatio-Temporal Perspective: An Interdisciplinary Approach to  
805 Interpret Archaeological Assemblages, in: Conrad, Nicolas.J. (Ed.), *Settlement Dynamics*  
806 *of the Middle Paleolithic and Middle Stone Age,* Tübingen Publications in Prehistory.  
807 Kerns, Tübingen, pp. 253–294.  
808  
809 Coil, R., 2016. *Spatial approaches to site formation and carnivore-hominin interaction at*  
810 *Dmanisi, Georgia.* (Ph.D. Dissertation). University of Minnesota.  
811  
812 Coil, R., Tappen, M., Ferring, R., Bukhsianidze, M., Nioradze, M., Lordkipanidze, D.,  
813 2020. Spatial patterning of the archaeological and paleontological assemblage at Dmanisi,  
814 Georgia: An analysis of site formation and carnivore-hominin interaction in Block 2.

815 Journal of Human Evolution 143, 102773. <https://doi.org/10.1016/j.jhevol.2020.102773>  
816  
817 Comber, J., 1967. Le Paléolithique de l'Ardèche dans son cadre bioclimatique.  
818 Imprimerie Delmas, Bordeaux.  
819  
820 Courbin, P., Brenet, M., Michel, A., Gravina, B., 2020. Spatial analysis of the late Middle  
821 Palaeolithic open-air site of Bout-des-Vergnes (Bergerac, Dordogne) based on lithic  
822 technology and refitting. *Journal of Archaeological Science: Reports* 32, 102373.  
823 <https://doi.org/10.1016/j.jasrep.2020.102373>  
824  
825 Cziesla, E., 1990. On refitting of stone artifacts, in: Cziesla, E., Eickhoff, S., Arts, N.,  
826 Winter (Eds.), *The Big Puzzle. International Symposium on Refitting Stone Artefacts.*  
827 *Studies in Modern Archaeology, Holos, Bonn*, pp. 9–44.  
828  
829 Daujeard, C., Vettese, D., Britton, K., Béarez, P., Boulbes, N., Crégut-Bonnoure, E.,  
830 Desclaux, E., Lateur, N., Pike-Tay, A., Rivals, F., Allué, E., Chacón, M.G., Puaud, S.,  
831 Richard, M., Courty, M.-A., Gallotti, R., Hardy, B., Bahain, J.J., Falguères, C., Pons-  
832 Branchu, E., Valladas, H., Moncel, M.-H., 2019. Neanderthal selective hunting of  
833 reindeer? The case study of Abri du Maras (south-eastern France). *Archaeol Anthropol*  
834 *Sci* 11, 985–1011. <https://doi.org/10.1007/s12520-017-0580-8>  
835  
836 de la Torre, I., Vanwezer, N., Benito-Calvo, A., Proffitt, T., Mora, R., 2019. Spatial and  
837 orientation patterns of experimental stone tool refits. *Archaeol Anthropol Sci* 11, 4569–  
838 4584. <https://doi.org/10.1007/s12520-018-0701-z>  
839  
840 Debard, E., 1988. Le Quaternaire du Bas-Vivarais d'après l'étude des remplissages  
841 d'avens, de porches de grottes et d'abris sous roche. *Dynamique sédimentaire,*  
842 *paléoclimatologie et chronologie. Travaux et Documents des Laboratoires de Géologie de*  
843 *Lyon* 103, 3–317.  
844  
845 Dell'Unto, N., Landeschi, G., 2022. *Archaeological 3D GIS*, 1st ed. Routledge, London.  
846 <https://doi.org/10.4324/9781003034131>  
847  
848 Dibble, H.L., Chase, P.G., McPherron, S.P., Tuffreau, A., 1997. Testing the Reality of a  
849 “Living Floor” with Archaeological Data. *Am. antiq.* 62, 629–651.  
850 <https://doi.org/10.2307/281882>  
851  
852 Ducke, B., 2012. Natives of a connected world: free and open source software in  
853 archaeology. *World Archaeology* 44, 571–579.  
854 <https://doi.org/10.1080/00438243.2012.743259>  
855  
856 ESRI, 2016. Que sont les données raster ? [WWW Document]. ArcGIS Desktop. URL  
857 [https://desktop.arcgis.com/fr/arcmap/10.3/manage-data/raster-and-images/what-is-raster-](https://desktop.arcgis.com/fr/arcmap/10.3/manage-data/raster-and-images/what-is-raster-data.htm)  
858 [data.htm](https://desktop.arcgis.com/fr/arcmap/10.3/manage-data/raster-and-images/what-is-raster-data.htm) (accessed 8.28.21).  
859  
860 Gabucio, M.J., Bargalló, A., Saladié, P., Romagnoli, F., Chacón, M.G., Vallverdú, J.,  
861 Vaquero, M., 2023. Using GIS and Geostatistical Techniques to Identify Neanderthal  
862 Campsites at archaeological level Ob at Abric Romani. *Archaeol Anthropol Sci* 15, 24.  
863 <https://doi.org/10.1007/s12520-023-01715-6>  
864

865 Galanidou, N., 2000. Patterns in Caves: Foragers, Horticulturists, and the Use of Space.  
866 *Journal of Anthropological Archaeology* 19, 243–275.  
867 <https://doi.org/10.1006/jaar.1999.0362>  
868

869 Getis, A., Ord, J.K., 1992. The Analysis of Spatial Association by Use of Distance  
870 Statistics. *Geographical Analysis* 24, 189–206. [https://doi.org/10.1111/j.1538-](https://doi.org/10.1111/j.1538-4632.1992.tb00261.x)  
871 [4632.1992.tb00261.x](https://doi.org/10.1111/j.1538-4632.1992.tb00261.x)  
872

873 Giusti, D., Turloukis, V., Konidaris, GeorgeE., Thompson, N., Karkanis, P.,  
874 Panagopoulou, E., Harvati, K., 2018. Beyond maps: Patterns of formation processes at the  
875 Middle Pleistocene open-air site of Marathousa 1, Megalopolis basin, Greece. *Quaternary*  
876 *International* 497, 137–153. <https://doi.org/10.1016/j.quaint.2018.01.041>  
877

878 Guillemot, P., 2021. Analyse spatiale des niveaux 4.1 et 4.2 de l'Abri du Maras (Ardèche,  
879 France), approche combinée : SIG et 3D. (M.Sc. Dissertation). Muséum national  
880 d'Histoire naturelle.  
881

882 Hardy, B.L., Moncel, M.-H., Daujeard, C., Fernandes, P., Béarez, P., Desclaux, E.,  
883 Chacon Navarro, M.G., Puaud, S., Gallotti, R., 2013. Impossible Neanderthals? Making  
884 string, throwing projectiles and catching small game during Marine Isotope Stage 4 (Abri  
885 du Maras, France). *Quaternary Science Reviews* 82, 23–40.  
886 <https://doi.org/10.1016/j.quascirev.2013.09.028>  
887

888 Hardy, B.L., Moncel, M.-H., Kerfant, C., Lebon, M., Bellot-Gurlet, L., Mélard, N., 2020.  
889 Direct evidence of Neanderthal fibre technology and its cognitive and behavioral  
890 implications. *Scientific Reports* 10, 4889. <https://doi.org/10.1038/s41598-020-61839-w>  
891

892 Henry, D., 2012. The palimpsest problem, hearth pattern analysis, and Middle Paleolithic  
893 site structure. *Quaternary International* 247, 246–266.  
894 <https://doi.org/10.1016/j.quaint.2010.10.013>  
895

896 Henry, D.O., Hietala, H.J., Rosen, A.M., Demidenko, Y.E., Usik, V.I., Armagan, T.L.,  
897 2004. Human Behavioral Organization in the Middle Paleolithic: Were Neanderthals  
898 Different? *American Anthropologist* 106, 17–31. <https://doi.org/10.1525/aa.2004.106.1.17>  
899

900 Howey, M.C.L., Brouwer Burg, M., 2017. Assessing the state of archaeological GIS  
901 research: Unbinding analyses of past landscapes. *Journal of Archaeological Science* 84, 1–  
902 9. <https://doi.org/10.1016/j.jas.2017.05.002>  
903

904 Ince, D.C., Hatton, L., Graham-Cumming, J., 2012. The case for open computer  
905 programs. *Nature* 482, 485–488. <https://doi.org/10.1038/nature10836>  
906

907 Jaillet, S., Sadier, B., Perazio, G., Delannoy, J.-J., 2014. Une brève histoire de la 3D en  
908 grotte. *Karstologia* 63, 3–20.  
909

910 Machado, J., Hernández, C.M., Mallol, C., Galván, B., 2013. Lithic production, site  
911 formation and Middle Palaeolithic palimpsest analysis: in search of human occupation  
912 episodes at Abric del Pastor Stratigraphic Unit IV (Alicante, Spain). *Journal of*  
913 *Archaeological Science* 40, 2254–2273. <https://doi.org/10.1016/j.jas.2013.01.002>  
914

- 915 Machado, J., Mayor, A., Hernández, C.M., Galván, B., 2019. Lithic refitting and the  
916 analysis of Middle Palaeolithic settlement dynamics: a high-temporal resolution example  
917 from El Pastor rock shelter (Eastern Iberia). *Archaeol Anthropol Sci* 11, 4539–4554.  
918 <https://doi.org/10.1007/s12520-019-00859-8>  
919
- 920 Malinsky-Buller, A., Hovers, E., Marder, O., 2011. Making time: ‘Living floors’,  
921 ‘palimpsests’ and site formation processes – A perspective from the open-air Lower  
922 Paleolithic site of Revadim Quarry, Israel. *Journal of Anthropological Archaeology* 30,  
923 89–101. <https://doi.org/10.1016/j.jaa.2010.11.002>  
924
- 925 Mallol, C., Hernández, C., 2016. Advances in palimpsest dissection. *Quaternary*  
926 *International* 417, 1–2. <https://doi.org/10.1016/j.quaint.2016.09.021>  
927
- 928 Marín, J., Daujeard, C., Saladié, P., Rodríguez-Hidalgo, A., Vettese, D., Rivals, F.,  
929 Boulbes, N., Crégut-Bonnoure, E., Lateur, N., Gallotti, R., Arbez, L., Puaud, S., Moncel,  
930 M.-H., 2020. Neanderthal faunal exploitation and settlement dynamics at the Abri du  
931 Maras, level 5 (south-eastern France). *Quaternary Science Reviews* 243, 106472.  
932 <https://doi.org/10.1016/j.quascirev.2020.106472>  
933
- 934 McCoy, M.D., Ladefoged, T.N., 2009. New Developments in the Use of Spatial  
935 Technology in Archaeology. *J Archaeol Res* 17, 263–295. [https://doi.org/10.1007/s10814-](https://doi.org/10.1007/s10814-009-9030-1)  
936 [009-9030-1](https://doi.org/10.1007/s10814-009-9030-1)  
937
- 938 Mellars, P., 1996. *The Neanderthal Legacy: An Archaeological Perspective from Western*  
939 *Europe*. Princeton University Press.  
940
- 941 Moncel, M.-H., Allué, E., Bailon, S., Barshay-Szmidt, C., Béarez, P., Crégut, É.,  
942 Daujeard, C., Desclaux, E., Debard, É., Lartigot-Campin, A.-S., Puaud, S., Roger, T.,  
943 2015. Evaluating the integrity of palaeoenvironmental and archaeological records in MIS  
944 5 to 3 karst sequences from southeastern France. *Quaternary International* 378, 22–39.  
945 <https://doi.org/10.1016/j.quaint.2013.12.009>  
946
- 947 Moncel, M.-H., Chacón, M.G., La Porta, A., Fernandes, P., Hardy, B., Gallotti, R., 2014.  
948 Fragmented reduction processes: Middle Palaeolithic technical behaviour in the Abri du  
949 Maras shelter, southeastern France. *Quaternary International* 350, 180–204.  
950 <https://doi.org/10.1016/j.quaint.2014.05.013>  
951
- 952 Moncel, M.-H., Chacón, M.G., Vettese, D., Courty, M.-A., Daujeard, C., Eixea, A.,  
953 Fernandes, P., Allué, E., Hardy, B., Rivals, F., Béarez, P., Gallotti, R., Puaud, S., 2021.  
954 Late Neanderthal short-term and specialized occupations at the Abri du Maras (South-East  
955 France, level 4.1, MIS 3). *Archaeol Anthropol Sci* 13, 45. [https://doi.org/10.1007/s12520-](https://doi.org/10.1007/s12520-021-01285-5)  
956 [021-01285-5](https://doi.org/10.1007/s12520-021-01285-5)  
957
- 958 Moncel, M.-H., Daujeard, C., Navarro, M., Vettese, D., Fernandes, P., Hardy, B., Puaud,  
959 S., Richard, M., Allué, E., Béarez, P., Boulbes, N., Britton, K., Courty, M.-A., Crégut, E.,  
960 Desclaux, E., Gallotti, R., Joannes-Boyau, R., Kerfant, C., Lateur, N., Falguères, C., 2018.  
961 L’Abri du Maras. À Saint-Martin d’Ardèche, des habitats néandertaliens du début du  
962 dernier glaciaire 35, 3–11.  
963
- 964 Moncel, M.-H., Gaillard, C., Patou-Mathis, M., 1994. L’abri du Maras (Ardèche) : une

965 nouvelle campagne de fouilles dans un site Paléolithique moyen (1993). *Bulletin de la*  
966 *Société préhistorique française* 91, 363–368. <https://doi.org/10.3406/bspf.1994.9786>  
967

968 Mora Torcal, R., Roy Sunyer, M., Martínez-Moreno, J., Benito-Calvo, A., Samper Carro,  
969 S., 2020. Inside the Palimpsest: Identifying Short Occupations in the 497D Level of Cova  
970 Gran (Iberia), in: Cascalheira, J., Picin, A. (Eds.), *Short-Term Occupations in Paleolithic*  
971 *Archaeology, Interdisciplinary Contributions to Archaeology*. Springer International  
972 Publishing, Cham, pp. 39–69. [https://doi.org/10.1007/978-3-030-27403-0\\_3](https://doi.org/10.1007/978-3-030-27403-0_3)  
973

974 Morin, A., Urban, J., Adams, P.D., Foster, I., Sali, A., Baker, D., Sliz, P., 2012. Shining  
975 Light into Black Boxes. *Science* 336, 159–160. <https://doi.org/10.1126/science.1218263>  
976

977 Neruda, P., 2017. GIS analysis of the spatial distribution of Middle Palaeolithic artefacts  
978 in Kůlna Cave (Czech Republic). *Quaternary International* 435, 58–76.  
979 <https://doi.org/10.1016/j.quaint.2015.10.028>  
980

981 Ord, J.K., Getis, A., 1995. Local Spatial Autocorrelation Statistics: Distributional Issues  
982 and an Application. *Geographical Analysis* 27, 286–306. [https://doi.org/10.1111/j.1538-](https://doi.org/10.1111/j.1538-4632.1995.tb00912.x)  
983 [4632.1995.tb00912.x](https://doi.org/10.1111/j.1538-4632.1995.tb00912.x)  
984

985 Orengo, H., 2015. Open source GIS and geospatial software in archaeology: towards their  
986 integration into everyday archaeological practice, in: Wilson, A.T., Edwards, B. (Eds.),  
987 *Open Source Archaeology: Ethics and Practice*. De Gruyter Open, Warsaw Berlin, pp. 64–  
988 82.  
989

990 Oron, M., Goren-Inbar, N., 2014. Mousterian intra-site spatial patterning at Quneitra,  
991 Golan Heights. *Quaternary International* 331, 186–202.  
992 <https://doi.org/10.1016/j.quaint.2013.04.013>  
993

994 Oxoli, D., Molinari, M., Brovelli, M., 2018. Hotspot Analysis, an open source GIS tool  
995 for exploratory spatial data analysis: application to the study of soil consumption in Italy.  
996 *Rendiconti Online della Società Geologica Italiana* 46, 82–87.  
997 <https://doi.org/10.3301/ROL.2018.56>  
998

999 Oxoli, D., Prestifilippo, G., Bertocchi, D., Zurbarán, M., 2017. Enabling spatial  
1000 autocorrelation mapping in QGIS: The hotspot analysis plugin. *Geoinformatica Ambientale*  
1001 *e Mineraria* 151, 45–50.  
1002

1003 Oxoli, D., Zurbarán, M.A., Shaji, S., Muthusamy, A.K., 2016. Hotspot analysis: a first  
1004 prototype Python plugin enabling exploratory spatial data analysis into QGIS. *PeerJ*  
1005 *Preprints* 4, e2204v4. <https://doi.org/10.7287/peerj.preprints.2204v4>  
1006

1007 Petraglia, M.D., Potts, R., 1994. Water Flow and the Formation of Early Pleistocene  
1008 Artifact Sites in Olduvai Gorge, Tanzania. *Journal of Anthropological Archaeology* 13,  
1009 228–254. <https://doi.org/10.1006/jaar.1994.1014>  
1010

1011 Pettitt, P.B., 1997. High resolution Neanderthals? Interpreting middle palaeolithic intrasite  
1012 spatial data. *World Archaeology* 29, 208–224.  
1013 <https://doi.org/10.1080/00438243.1997.9980374>  
1014

1015 Picin, A., Cascalheira, J., 2020. Introduction to Short-Term Occupations in Palaeolithic  
1016 Archaeology, in: Cascalheira, J., Picin, A. (Eds.), Short-Term Occupations in Paleolithic  
1017 Archaeology, Interdisciplinary Contributions to Archaeology. Springer International  
1018 Publishing, Cham, pp. 1–15. [https://doi.org/10.1007/978-3-030-27403-0\\_1](https://doi.org/10.1007/978-3-030-27403-0_1)  
1019

1020 Puaud, S., Nowak, M., Pont, S., Moncel, M.-H., 2015. Minéraux volcaniques et alpins à  
1021 l’abri du Maras (Ardèche, France) : témoins de vents catabatiques dans la vallée du Rhône  
1022 au Pléistocène supérieur. *Comptes Rendus Palevol* 14, 331–341.  
1023 <https://doi.org/10.1016/j.crpv.2015.02.007>  
1024

1025 QGIS.org, 2021. QGIS Geographic Information System.  
1026

1027 Reeves, J.S., McPherron, S.P., Aldeias, V., Dibble, H.L., Goldberg, P., Sandgathe, D.,  
1028 Turq, A., 2019. Measuring spatial structure in time-averaged deposits insights from Roc  
1029 de Marsal, France. *Archaeol Anthropol Sci* 11, 5743–5762.  
1030 <https://doi.org/10.1007/s12520-019-00871-y>  
1031

1032 Richard, M., Falguères, C., Pons-Branchu, E., Bahain, J.-J., Voinchet, P., Lebon, M.,  
1033 Valladas, H., Dolo, J.-M., Puaud, S., Rué, M., Daujeard, C., Moncel, M.-H., Raynal, J.-P.,  
1034 2015. Contribution of ESR/U-series dating to the chronology of late Middle Palaeolithic  
1035 sites in the middle Rhône valley, southeastern France. *Quaternary Geochronology, LED14*  
1036 *Proceedings* 30, 529–534. <https://doi.org/10.1016/j.quageo.2015.06.002>  
1037

1038 Richard, M., Pons-Branchu, E., Genuite, K., Jaillet, S., Joannes-Boyau, R., Wang, N.,  
1039 Genty, D., Cheng, H., Price, G.J., Pierre, M., Dapoigny, A., Falguères, C., Tombret, O.,  
1040 Voinchet, P., Bahain, J.-J., Moncel, M.-H., 2021. Timing of Neanderthal occupations in  
1041 the southeastern margins of the Massif Central (France): A multi-method approach.  
1042 *Quaternary Science Reviews* 273, 107241.  
1043 <https://doi.org/10.1016/j.quascirev.2021.107241>  
1044

1045 Richards-Rissetto, H., 2017. What can GIS + 3D mean for landscape archaeology?  
1046 *Journal of Archaeological Science* 84, 10–21. <https://doi.org/10.1016/j.jas.2017.05.005>  
1047

1048 Romagnoli, F., Vaquero, M., 2016. Quantitative stone tools intra-site points and  
1049 orientation patterns of a Middle Palaeolithic living floor: A GIS multi-scalar spatial and  
1050 temporal approach. *Quartär* 63, 47–60. [https://doi.org/10.7485/QU63\\_3](https://doi.org/10.7485/QU63_3)  
1051

1052 Sánchez-Romero, L., Benito-Calvo, A., Marín-Arroyo, A.B., Agudo-Pérez, L.,  
1053 Karampaglidis, T., Rios-Garaizar, J., 2020. New insights for understanding spatial  
1054 patterning and formation processes of the Neanderthal occupation in the Amalda I cave  
1055 (Gipuzkoa, Spain). *Sci Rep* 10, 8733. <https://doi.org/10.1038/s41598-020-65364-8>  
1056

1057 Sánchez-Romero, L., Benito-Calvo, A., Pérez-González, A., Santonja, M., 2016.  
1058 Assessment of Accumulation Processes at the Middle Pleistocene Site of Ambrona (Soria,  
1059 Spain). Density and Orientation Patterns in Spatial Datasets Derived from Excavations  
1060 Conducted from the 1960s to the Present. *PLoS ONE* 11, e0167595.  
1061 <https://doi.org/10.1371/journal.pone.0167595>  
1062

1063 Sánchez-Romero, L., Benito-Calvo, A., Rios-Garaizar, J., 2021. Defining and  
1064 Characterising Clusters in Palaeolithic Sites: a Review of Methods and Constraints. *J*

1065 Archaeol Method Theory. <https://doi.org/10.1007/s10816-021-09524-8>  
1066  
1067 Sañudo, P., Vallverdú-Poch, J., Canals, A., 2012. Spatial Patterns in Level J, in: Carbonell  
1068 i Roura, E. (Ed.), High Resolution Archaeology and Neanderthal Behavior, Vertebrate  
1069 Paleobiology and Paleoanthropology. Springer Netherlands, Dordrecht, pp. 47–76.  
1070 [https://doi.org/10.1007/978-94-007-3922-2\\_3](https://doi.org/10.1007/978-94-007-3922-2_3)  
1071  
1072 Spagnolo, V., Marciani, G., Aureli, D., Berna, F., Toniello, G., Astudillo, F., Boschin, F.,  
1073 Boscato, P., Ronchitelli, A., 2019. Neanderthal activity and resting areas from  
1074 stratigraphic unit 13 at the Middle Palaeolithic site of Oscurusciuto (Ginosa - Taranto,  
1075 Southern Italy). *Quaternary Science Reviews* 217, 169–193.  
1076 <https://doi.org/10.1016/j.quascirev.2018.06.024>  
1077  
1078 Spagnolo, V., Marciani, G., Aureli, D., Martini, I., Boscato, P., Boschin, F., Ronchitelli,  
1079 A., 2020. Climbing the time to see Neanderthal behaviour’s continuity and discontinuity:  
1080 SU 11 of the Oscurusciuto Rockshelter (Ginosa, Southern Italy). *Archaeol Anthropol Sci*  
1081 12, 54. <https://doi.org/10.1007/s12520-019-00971-9>  
1082  
1083 Stavrova, T., Borel, A., Daujeard, C., Vettese, D., 2019. A GIS based approach to long  
1084 bone breakage patterns derived from marrow extraction. *PLoS ONE* 14, e0216733.  
1085 <https://doi.org/10.1371/journal.pone.0216733>  
1086  
1087 Vaquero, M., 2008. The history of stones: behavioural inferences and temporal resolution  
1088 of an archaeological assemblage from the Middle Palaeolithic. *Journal of Archaeological*  
1089 *Science* 35, 3178–3185. <https://doi.org/10.1016/j.jas.2008.07.006>  
1090  
1091 Vaquero, M., Chacón, M.G., García-Antón, M.D., Gómez de Soler, B., Martínez, K.,  
1092 Cuartero, F., 2012. Time and space in the formation of lithic assemblages: The example of  
1093 Abric Romaní Level J. *Quaternary International* 247, 162–181.  
1094 <https://doi.org/10.1016/j.quaint.2010.12.015>  
1095  
1096 Vaquero, M., Fernández-Laso, M.C., Chacón, M.G., Romagnoli, F., Rosell, J., Sañudo, P.,  
1097 2017. Moving things: Comparing lithic and bone refits from a Middle Paleolithic site.  
1098 *Journal of Anthropological Archaeology* 48, 262–280.  
1099 <https://doi.org/10.1016/j.jaa.2017.09.001>  
1100  
1101 Vaquero, M., Pastó, I., 2001. The Definition of Spatial Units in Middle Palaeolithic Sites:  
1102 The Hearth-Related Assemblages. *Journal of Archaeological Science* 28, 1209–1220.  
1103 <https://doi.org/10.1006/jasc.2001.0656>  
1104  
1105 Vaquero, M., Romagnoli, F., Bargalló, A., Chacón, M.G., Gómez de Soler, B., Picin, A.,  
1106 Carbonell, E., 2019. Lithic refitting and intrasite artifact transport: a view from the Middle  
1107 Paleolithic. *Archaeol Anthropol Sci* 11, 4491–4513. [https://doi.org/10.1007/s12520-019-](https://doi.org/10.1007/s12520-019-00832-5)  
1108 [00832-5](https://doi.org/10.1007/s12520-019-00832-5)  
1109  
1110 Vaquero, M., Vallverdú, J., Rosell, J., Pastó, I., Allué, E., 2001. Neandertal Behavior at  
1111 the Middle Palaeolithic Site of Abric Romaní, Capellades, Spain. *Journal of Field*  
1112 *Archaeology* 28, 93–114. <https://doi.org/10.1179/jfa.2001.28.1-2.93>  
1113  
1114 Vettese, D., Borel, A., Blasco, R., Chevillard, L., Stavrova, T., Thun Hohenstein, U.,



1115 Arzarello, M., Moncel, M.-H., Daujeard, C., 2022. New evidence of Neandertal butchery  
1116 traditions through the marrow extraction in southwestern Europe (MIS 5–3). PLoS ONE  
1117 17, e0271816. <https://doi.org/10.1371/journal.pone.0271816>  
1118

1119 Vettese, D., Daujeard, C., Blasco, R., Borel, A., Caceres, I., Moncel, M.H., 2017.  
1120 Neandertal long bone breakage process: Standardized or random patterns? The example of  
1121 Abri du Maras (Southeastern France, MIS 3). *Journal of Archaeological Science: Reports*  
1122 13, 151–163. <https://doi.org/10.1016/j.jasrep.2017.03.029>  
1123

1124 Vignes, M.-P., 2021. Approche multidisciplinaire des stratégies de subsistance des  
1125 Néandertaliens à l’Abri du Maras (Ardèche): Archéozoologie, taphonomie et analyse  
1126 spatiale de la grande faune du niveau 4.2 (MIS 3). (M.Sc. Dissertation). Muséum national  
1127 d’Histoire naturelle.  
1128

1129 Westoby, M.J., Brasington, J., Glasser, N.F., Hambrey, M.J., Reynolds, J.M., 2012.  
1130 ‘Structure-from-Motion’ photogrammetry: A low-cost, effective tool for geoscience  
1131 applications. *Geomorphology* 179, 300–314.  
1132 <https://doi.org/10.1016/j.geomorph.2012.08.021>  
1133

1134 Whitley, T.G., 2017. Geospatial analysis as experimental archaeology. *Journal of*  
1135 *Archaeological Science* 84, 103–114. <https://doi.org/10.1016/j.jas.2017.05.008>  
1136  
1137

#### 1138 **Figure caption list**

1139

1140 **Figure 1.** Methodology used for palaeotopographic rendering and analysis of levels 4.1 and  
1141 4.2.  
1142

1143 **Figure 2.** Spatial patterns of lithics, bones and fire-related artefacts from Maras level 4.1.  
1144 Hotspot analysis applied to lithic artefacts (A); hotspot analysis applied to faunal remains (B);  
1145 spatial analysis of fire-related artefacts: kernel density of burnt lithics, hotspot analysis of  
1146 charcoal remains and ash lenses scattering (C).  
1147

1148 **Figure 3.** Hotspot analysis of the two RMUs with the most pieces: hotspot analysis of the  
1149 RMU flint-13 (A), hotspot analysis of the RMU quartz-5 (B) from Maras level 4.1.  
1150

1151 **Figure 4.** Kernel density of tool kits from Maras level 4.1.  
1152

1153 **Figure 5.** Hotspot analysis of cortical flakes from Maras level 4.1.  
1154

1155 **Figure 6.** Hotspot analysis of lithic tools from Maras level 4.1.  
1156

1157 **Figure 7.** Hotspot analysis according to the length of lithic artefacts from Maras level 4.1.  
1158

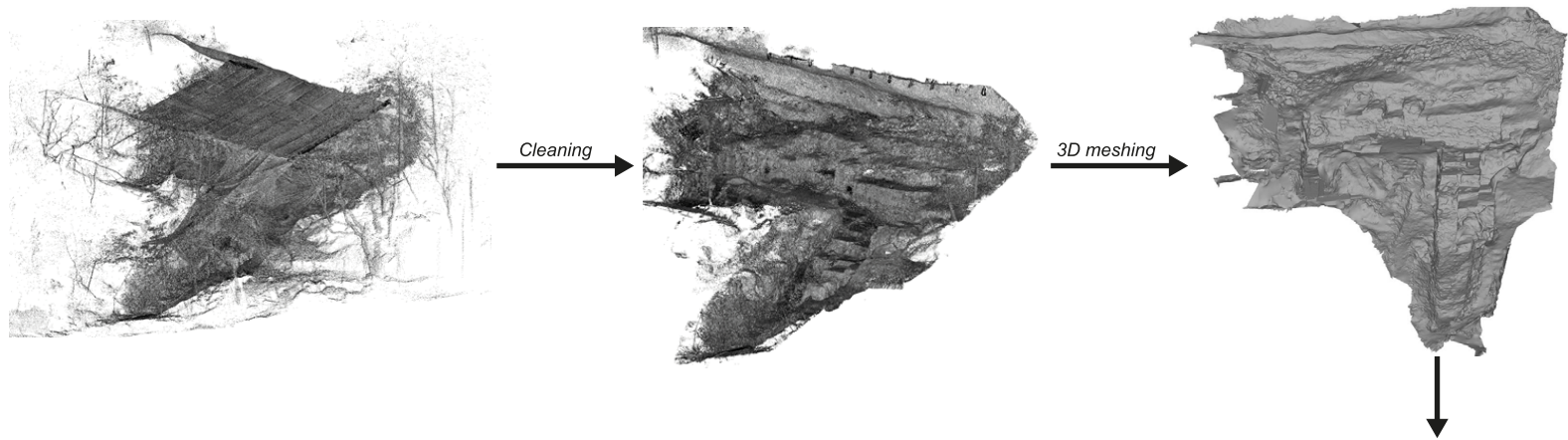
1159 **Figure 8.** Spatial patterns of lithics, bones and fire-related artefacts from Maras level 4.2.  
1160 Hotspot analysis applied to lithic artefacts (A); hotspot analysis applied to faunal remains (B);  
1161 spatial analysis of fire-related artefacts: kernel density of burnt lithics, hotspot analysis of  
1162 charcoal remains and ash lenses scattering (C).  
1163

1164 **Figure 9.** Hotspot analysis of cortical flakes from Maras level 4.2.

1165  
1166 **Figure 10.** Hotspot analysis of lithic tools from Maras level 4.2.  
1167  
1168 **Figure 11.** Hotspot analysis of cores from Maras level 4.2.  
1169  
1170 **Figure 12.** Hotspot analysis according to the length of lithic artefacts from Maras level 4.2  
1171 (dotted circles represent clusters in the disturbed areas of the site).  
1172  
1173 **Figure 13.** Palaeotopography of level 4.1: palaeosurface rendering of level 4.1 in the 3D mesh  
1174 model of the Abri du Maras (A), DTM of the surface of level 4.1 with N-S and W-E  
1175 palaeotopographic profiles.  
1176  
1177 **Figure 14.** Palaeotopography of level 4.2: palaeosurface rendering of level 4.2 within the 3D  
1178 mesh model of the Abri du Maras (A), DTM of the surface of level 4.2 with N-S and W-E  
1179 palaeotopographic profiles.  
1180  
1181 **Figure 15.** Spatial patterns identified from the spatial analysis of Maras level 4.1 (A) & level  
1182 4.2 (B).

Figure 1

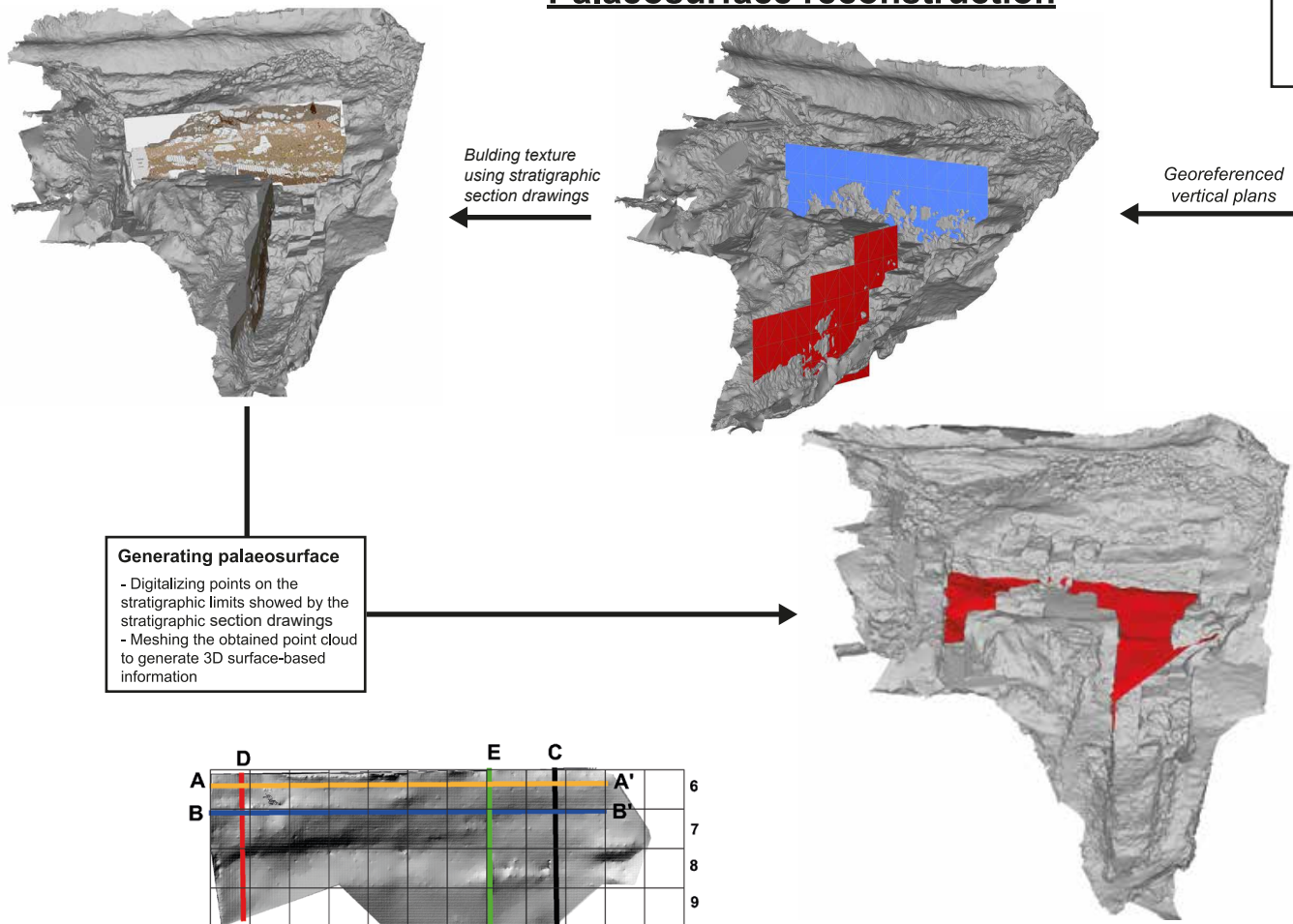
### Preliminary processing on the 3D model



**Modification of the coordinate system**

- Rotation
- Translation in X, Y and Z coordinates

### Palaeosurface reconstruction



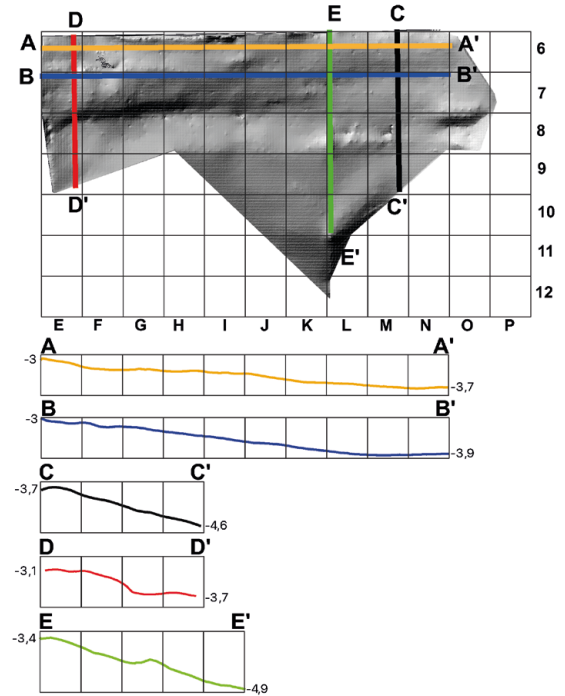
**Generating palaeosurface**

- Digitalizing points on the stratigraphic limits showed by the stratigraphic section drawings
- Meshing the obtained point cloud to generate 3D surface-based information

### Analysing palaeotopography in 2D

**QGIS analysis**

- Rasterising 3D surface into DTM
- Saving as TIF file
- Importing into QGIS
- Using profil tool



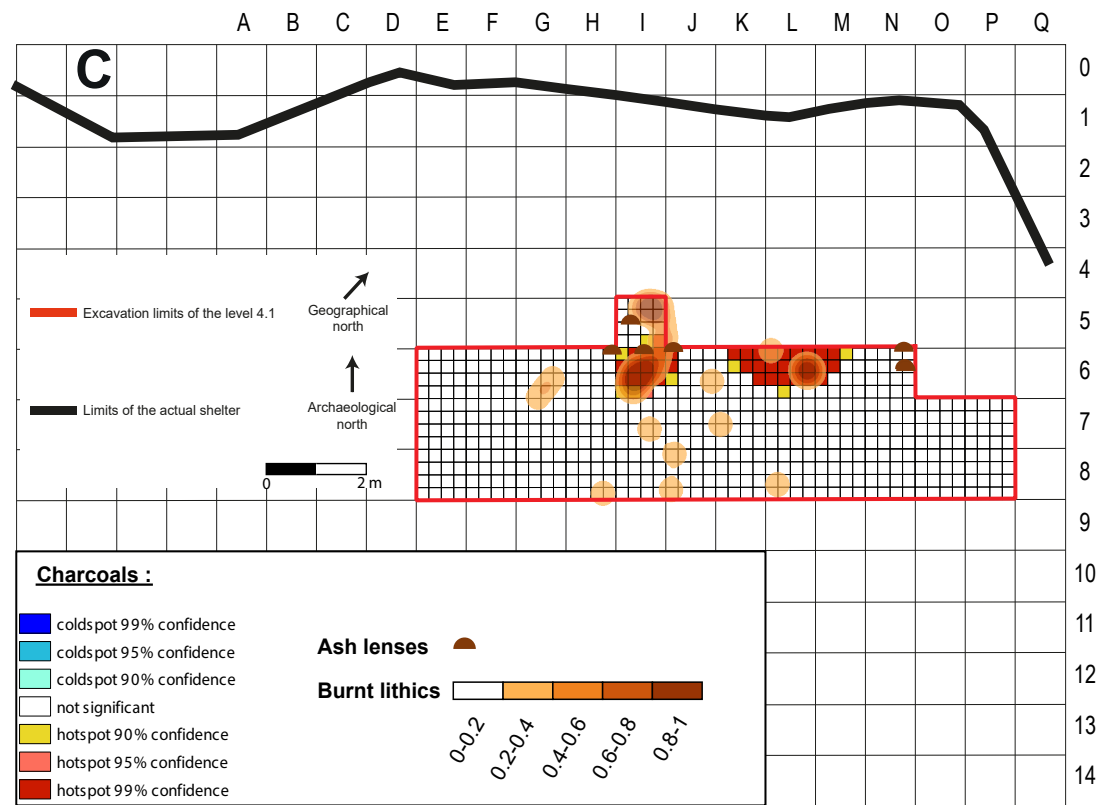
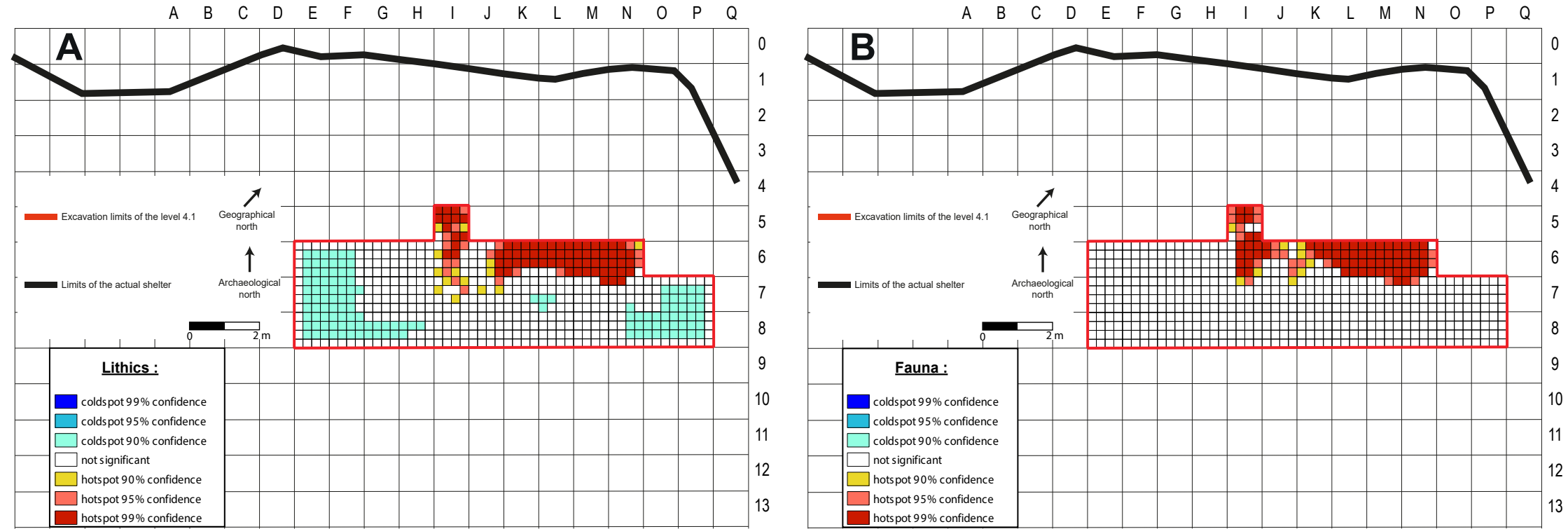
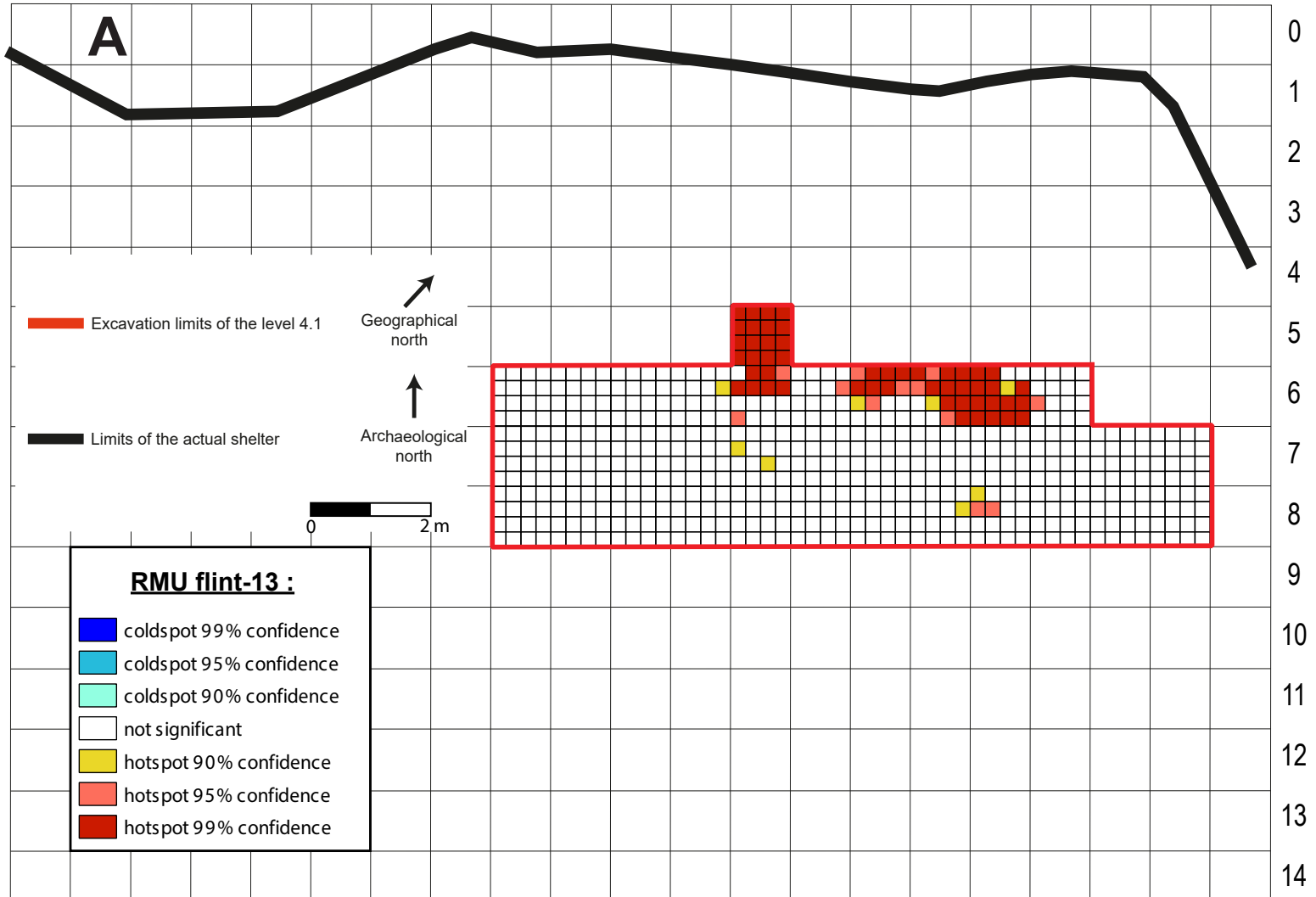


Figure 2

Figure 3

A B C D E F G H I J K L M N O P Q



A B C D E F G H I J K L M N O P Q

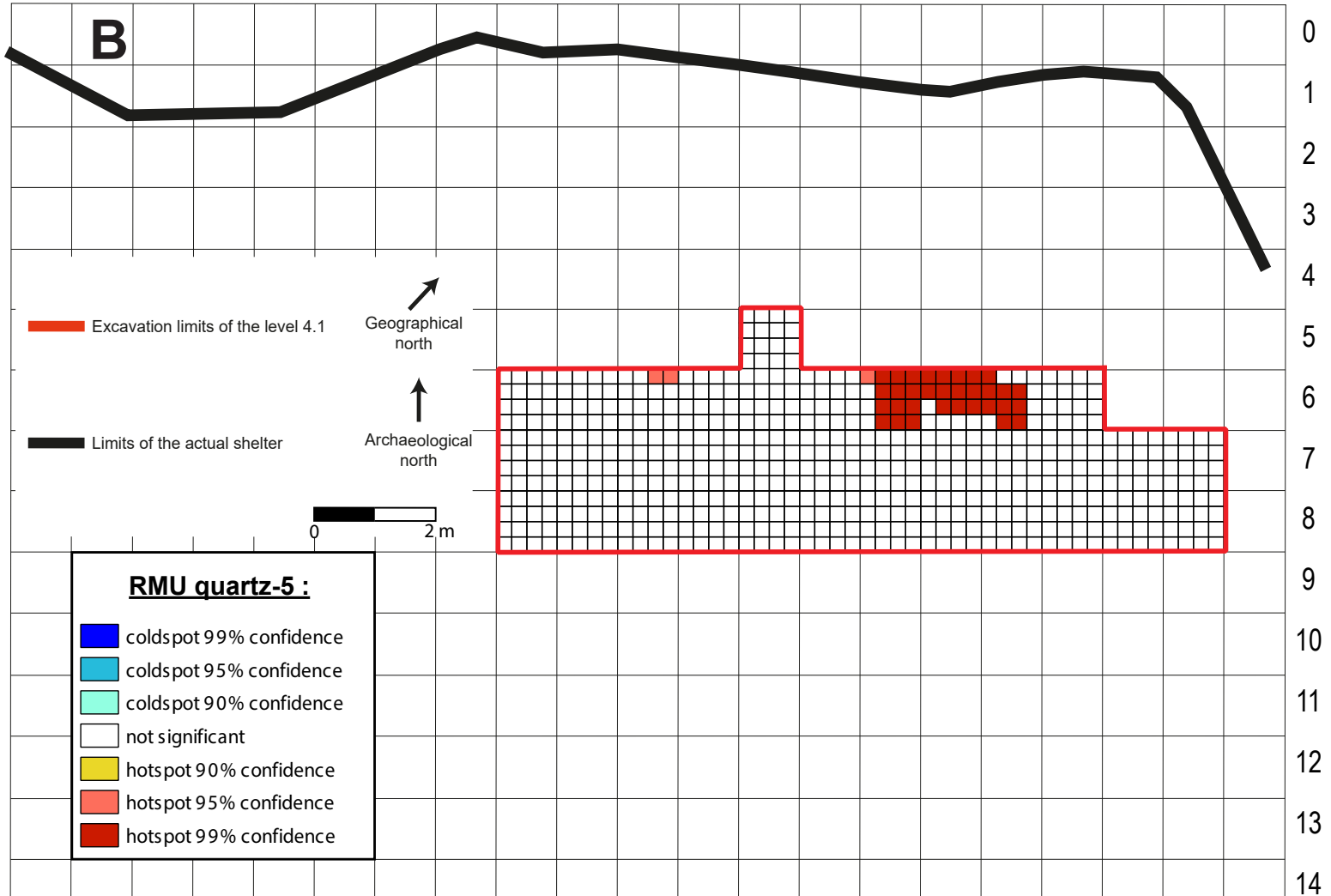


Figure 4

A B C D E F G H I J K L M N O P Q

0  
1  
2  
3  
4  
5  
6  
7  
8  
9  
10  
11  
12  
13  
14

Excavation limits of the level 4.1

Geographical north

Limits of the actual shelter

Archaeological north

0 2 m

Too kits



0-0.2  
0.2-0.4  
0.4-0.6  
0.6-0.8  
0.8-1

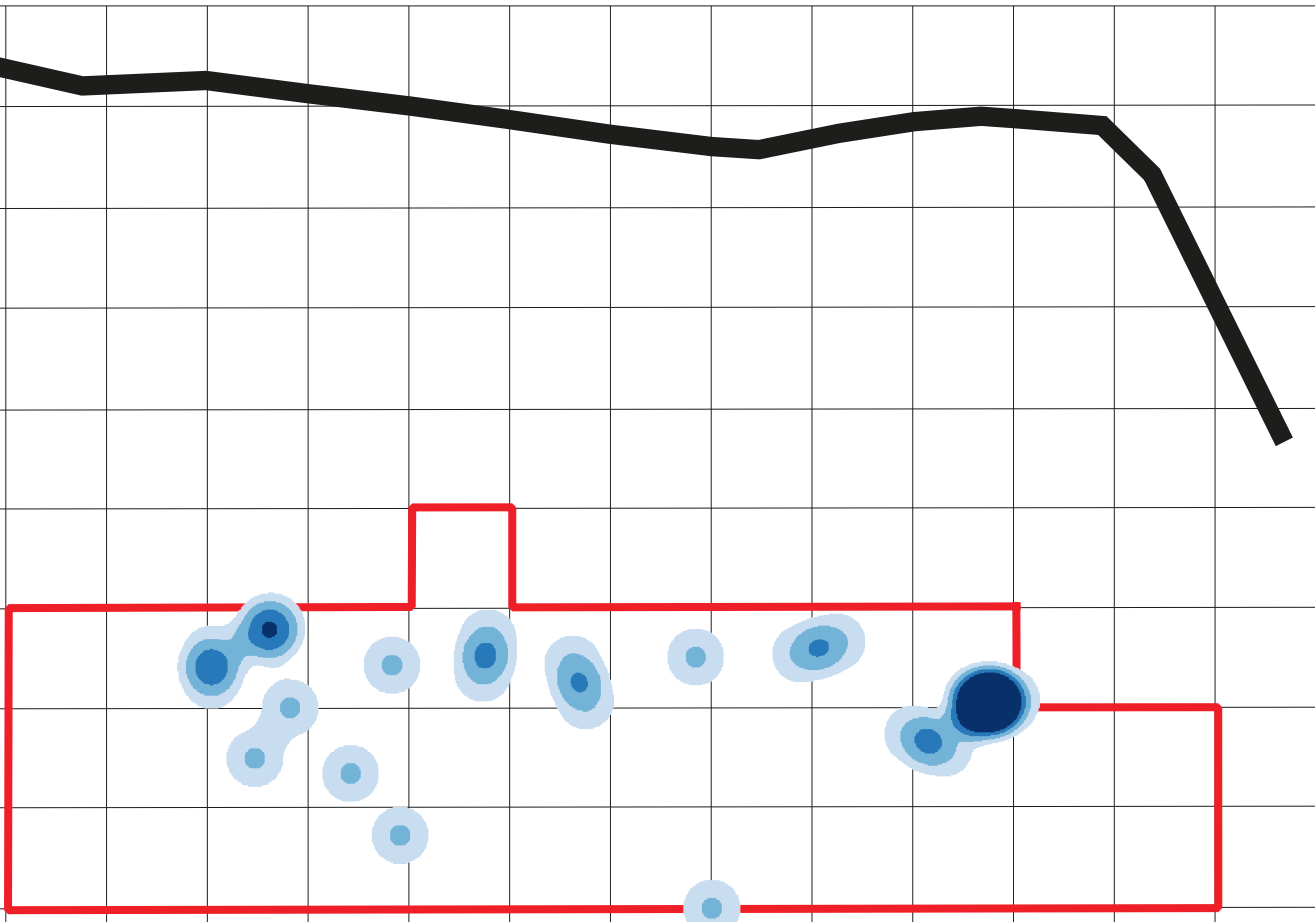


Figure 5

A B C D E F G H I J K L M N O P Q

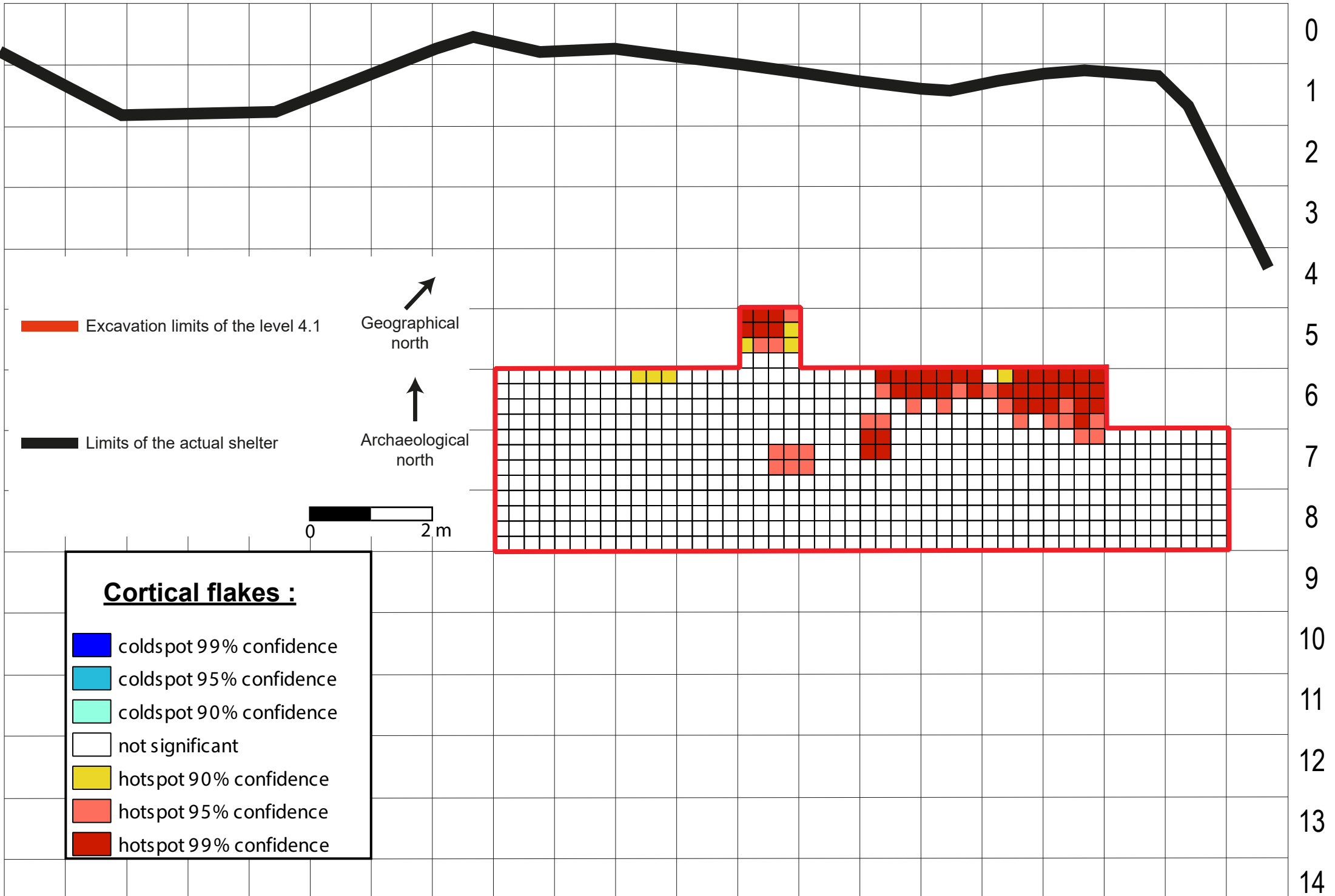
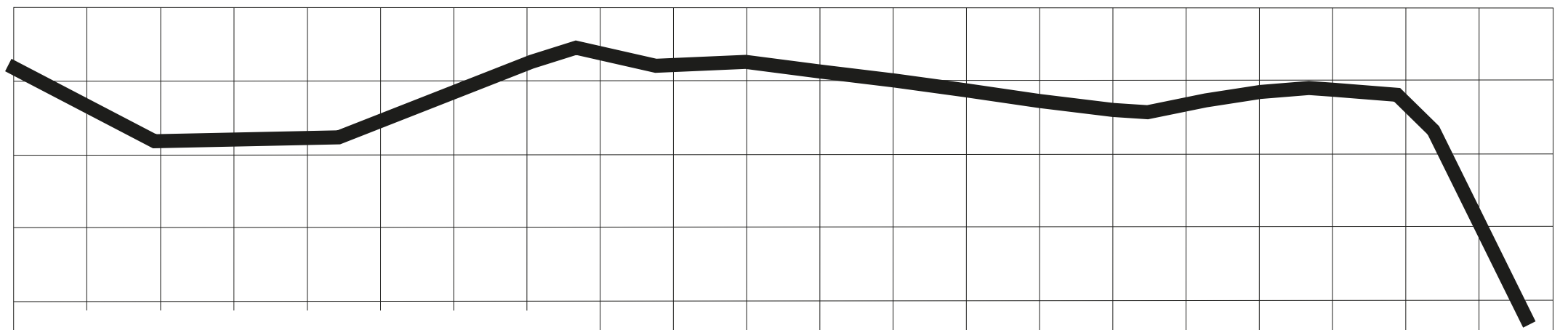


Figure 6

A B C D E F G H I J K L M N O P Q



Excavation limits of the level 4.1

Geographical north

Limits of the actual shelter

Archaeological north

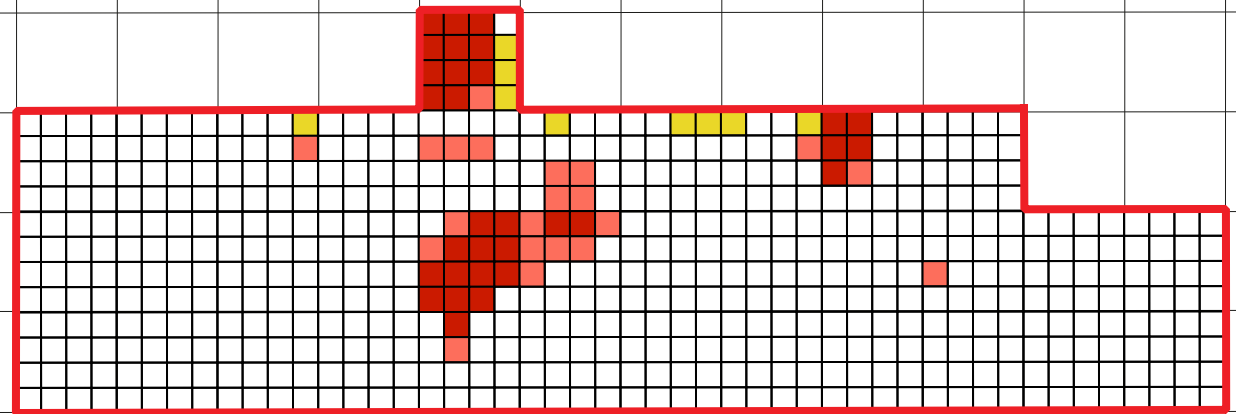
This block contains a legend for the excavation limits and directions. It includes a red line segment labeled 'Excavation limits of the level 4.1', an arrow pointing up-right labeled 'Geographical north', a thick black line segment labeled 'Limits of the actual shelter', and an arrow pointing up labeled 'Archaeological north'.



**Lithic tools :**

- coldspot 99% confidence
- coldspot 95% confidence
- coldspot 90% confidence
- not significant
- hotspot 90% confidence
- hotspot 95% confidence
- hotspot 99% confidence

This block contains a legend for lithic tool confidence levels. It lists seven categories with corresponding color swatches: coldspot 99% confidence (blue), coldspot 95% confidence (light blue), coldspot 90% confidence (light green), not significant (white), hotspot 90% confidence (yellow), hotspot 95% confidence (light red), and hotspot 99% confidence (dark red).



0  
1  
2  
3  
4  
5  
6  
7  
8  
9  
10  
11  
12  
13  
14



Figure 7

A B C D E F G H I J K L M N O P Q

0  
1  
2  
3  
4  
5  
6  
7  
8  
9  
10  
11  
12  
13  
14

Excavation limits of the level 4.1

Geographical north

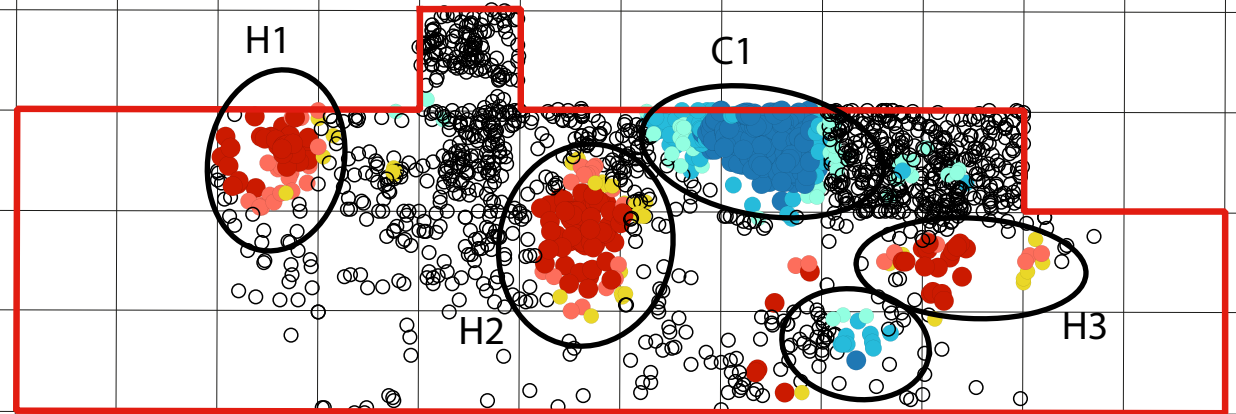
Limits of the actual shelter

Archaeological north

0 2 m

**Length:**

- coldspot 99% confidence
- coldspot 95% confidence
- coldspot 90% confidence
- not significant
- hotspot 90% confidence
- hotspot 95% confidence
- hotspot 99% confidence



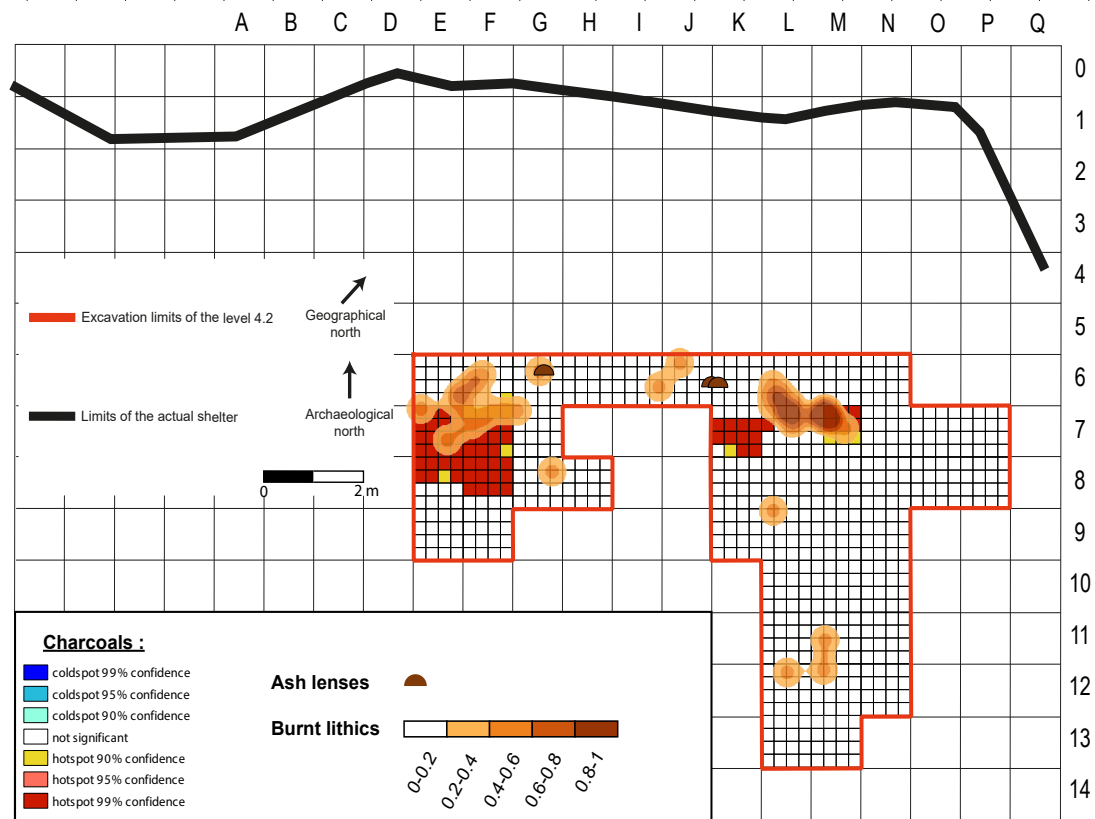
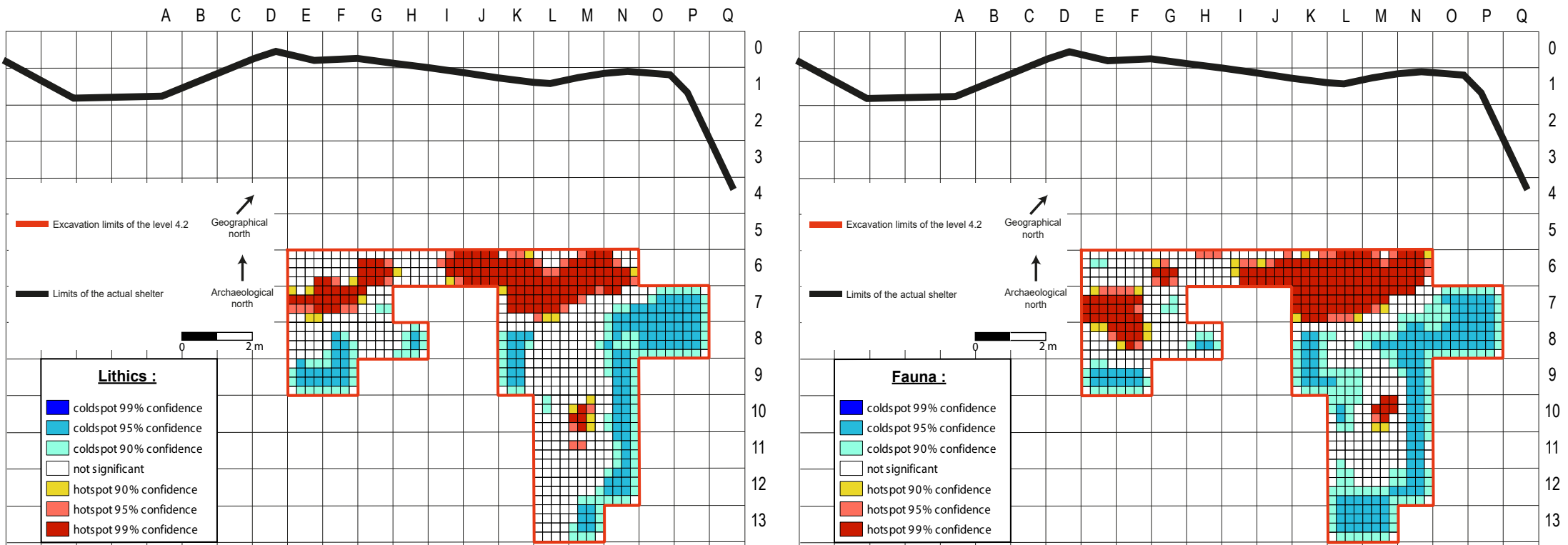


Figure 8

Figure 9

A B C D E F G H I J K L M N O P Q

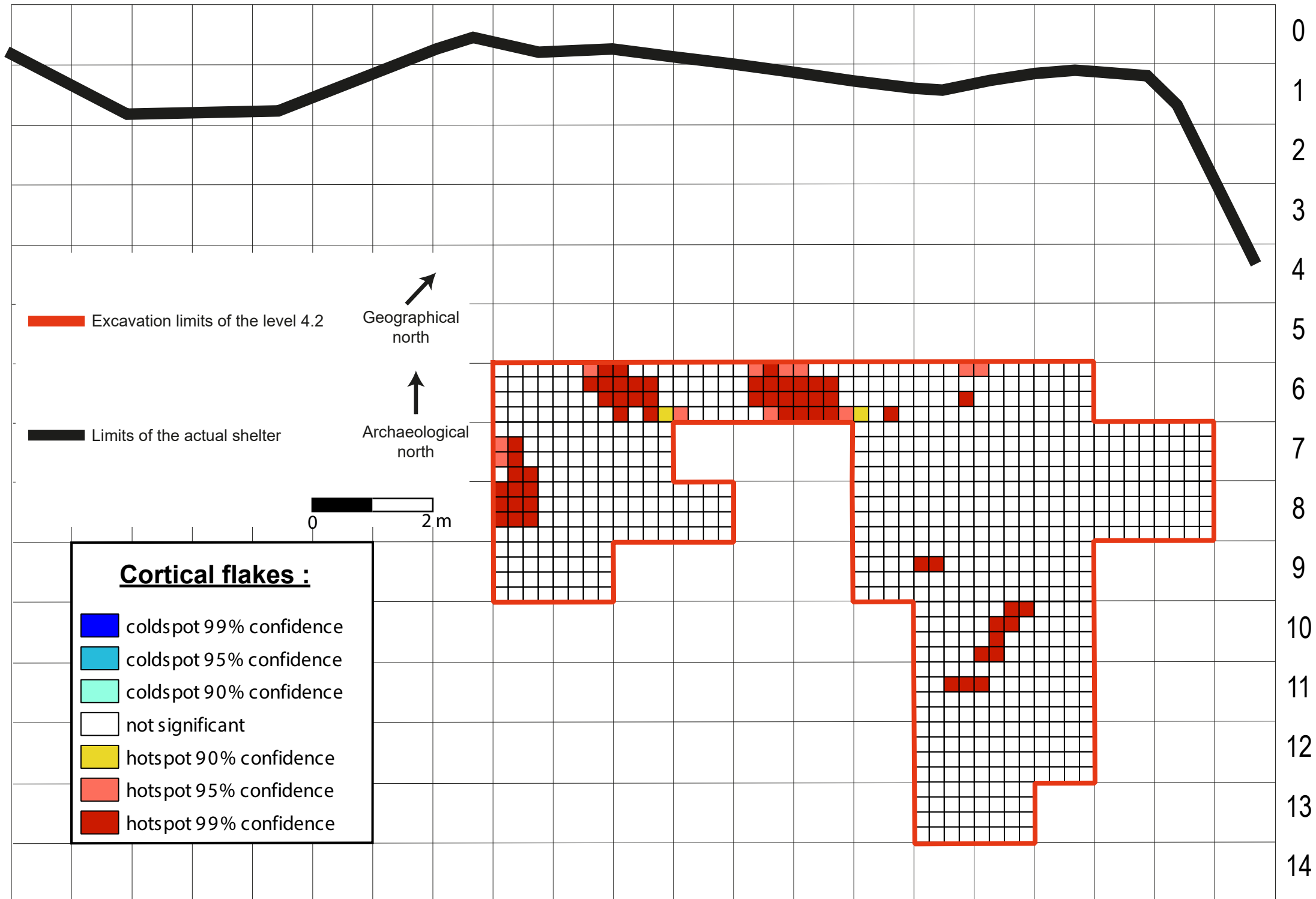


Figure 10

A B C D E F G H I J K L M N O P Q

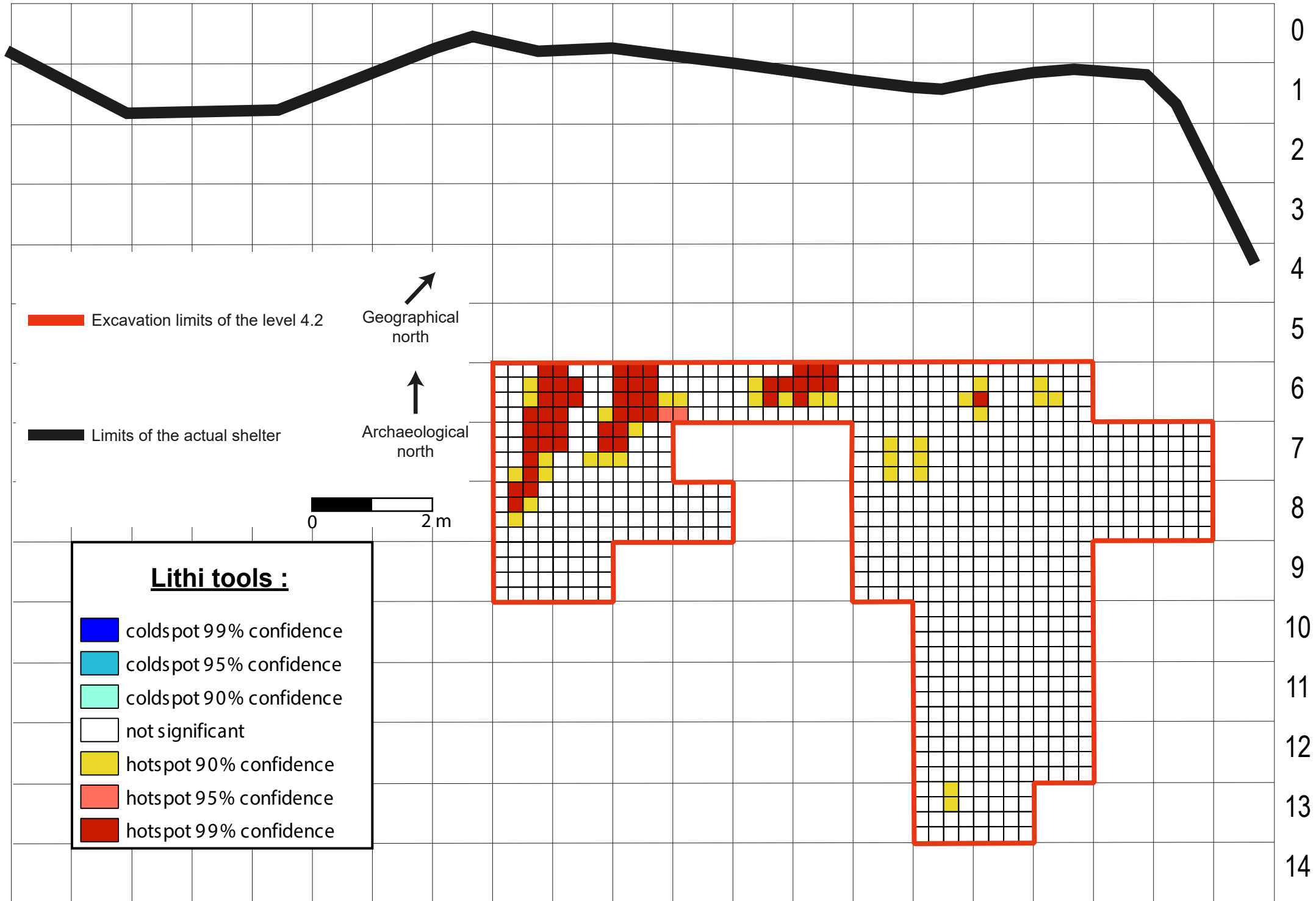


Figure 11

A B C D E F G H I J K L M N O P Q

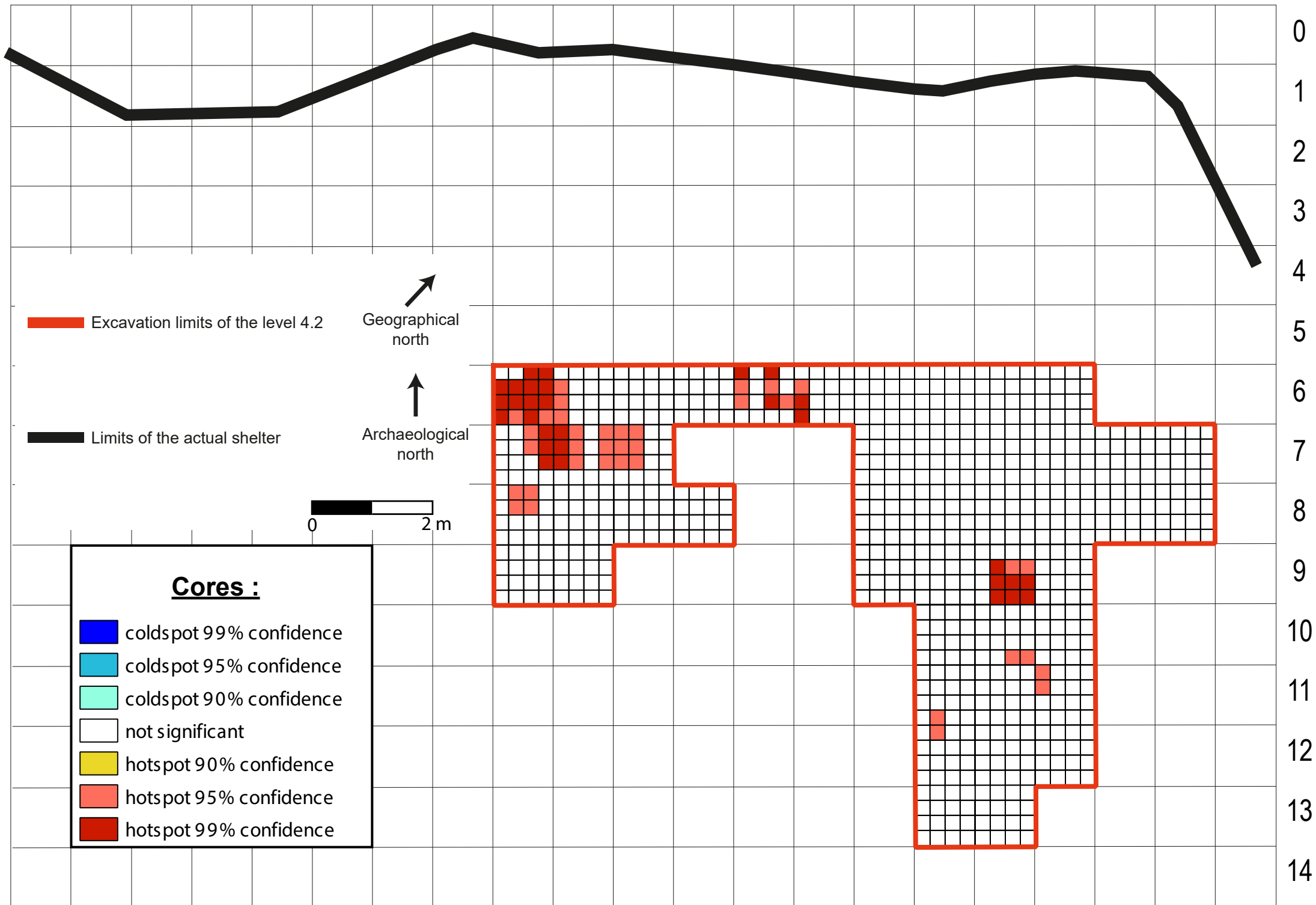
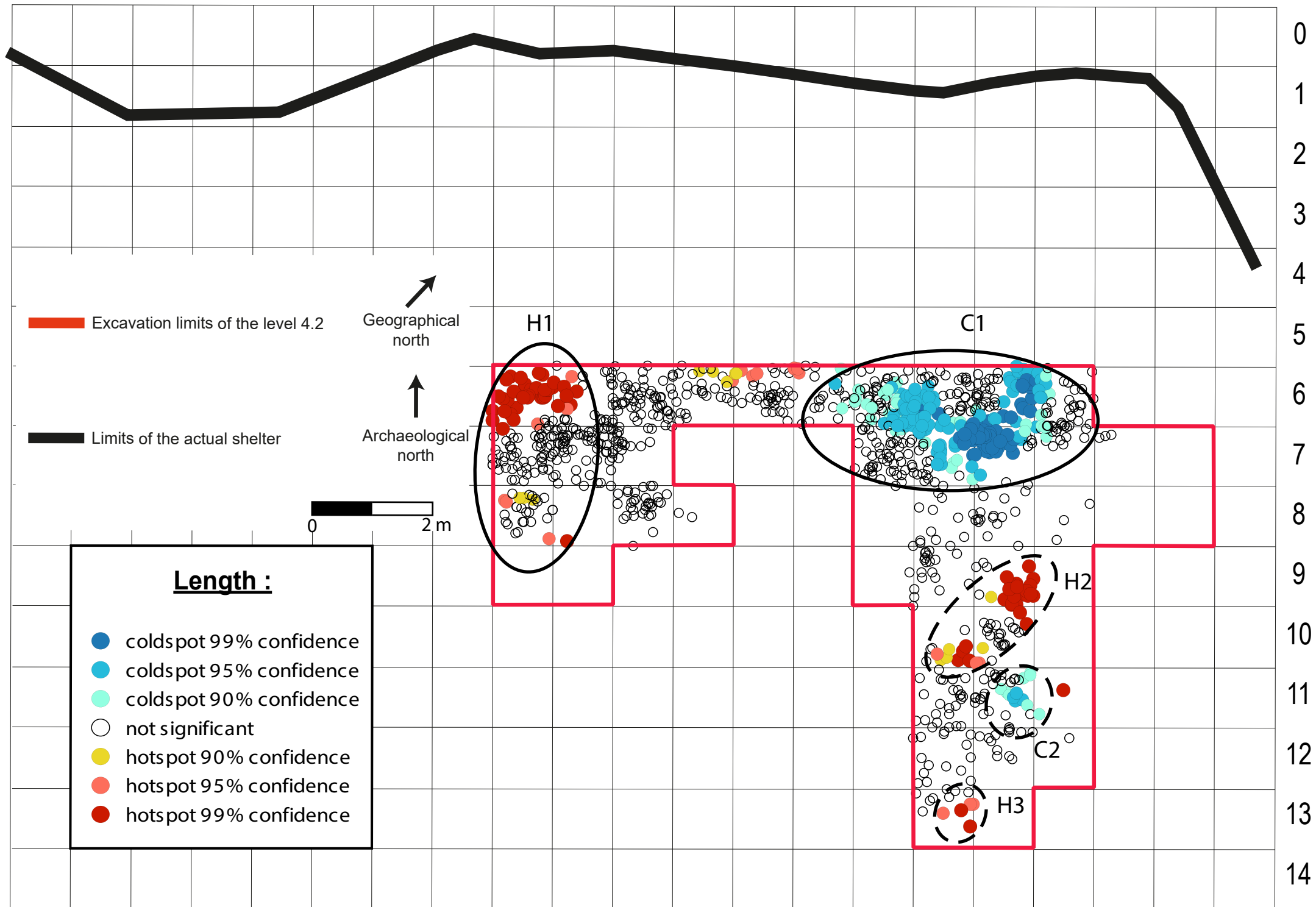


Figure 12

A B C D E F G H I J K L M N O P Q



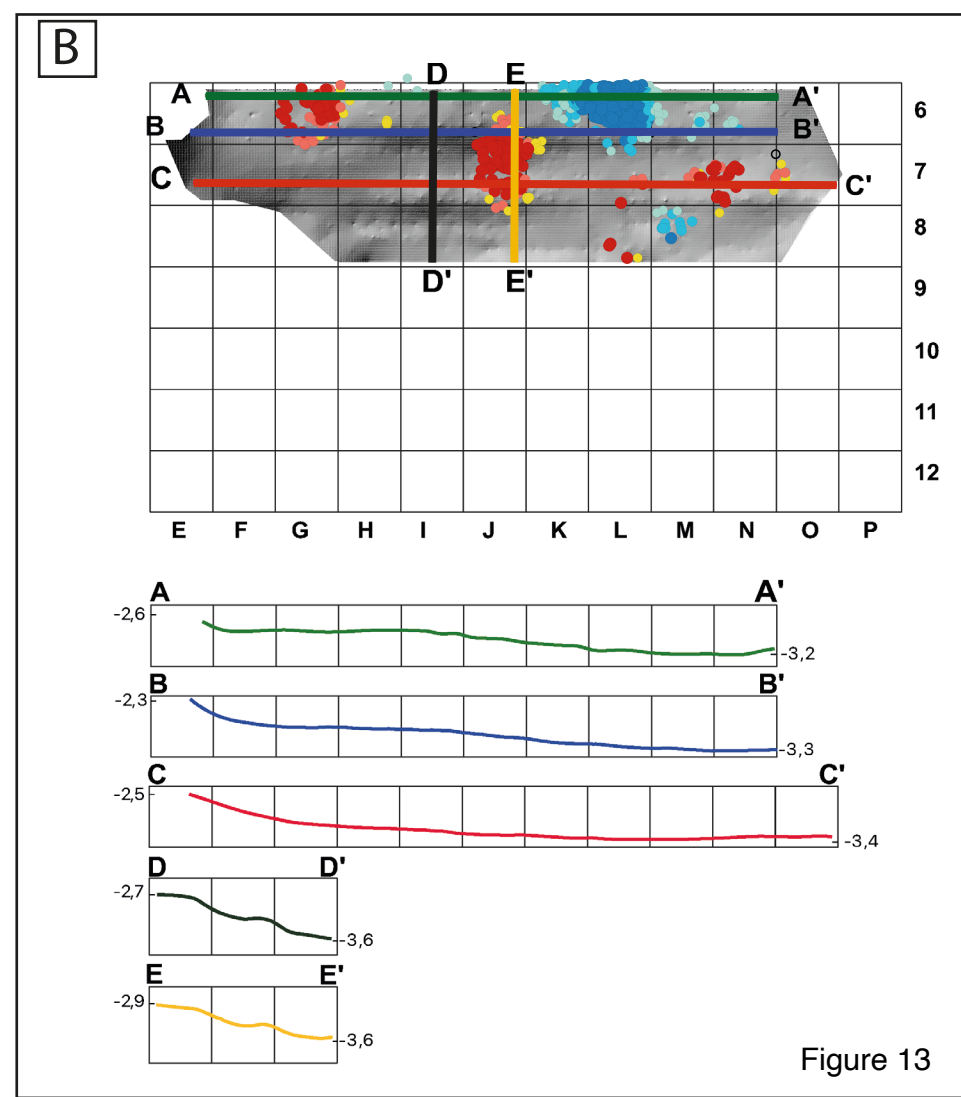
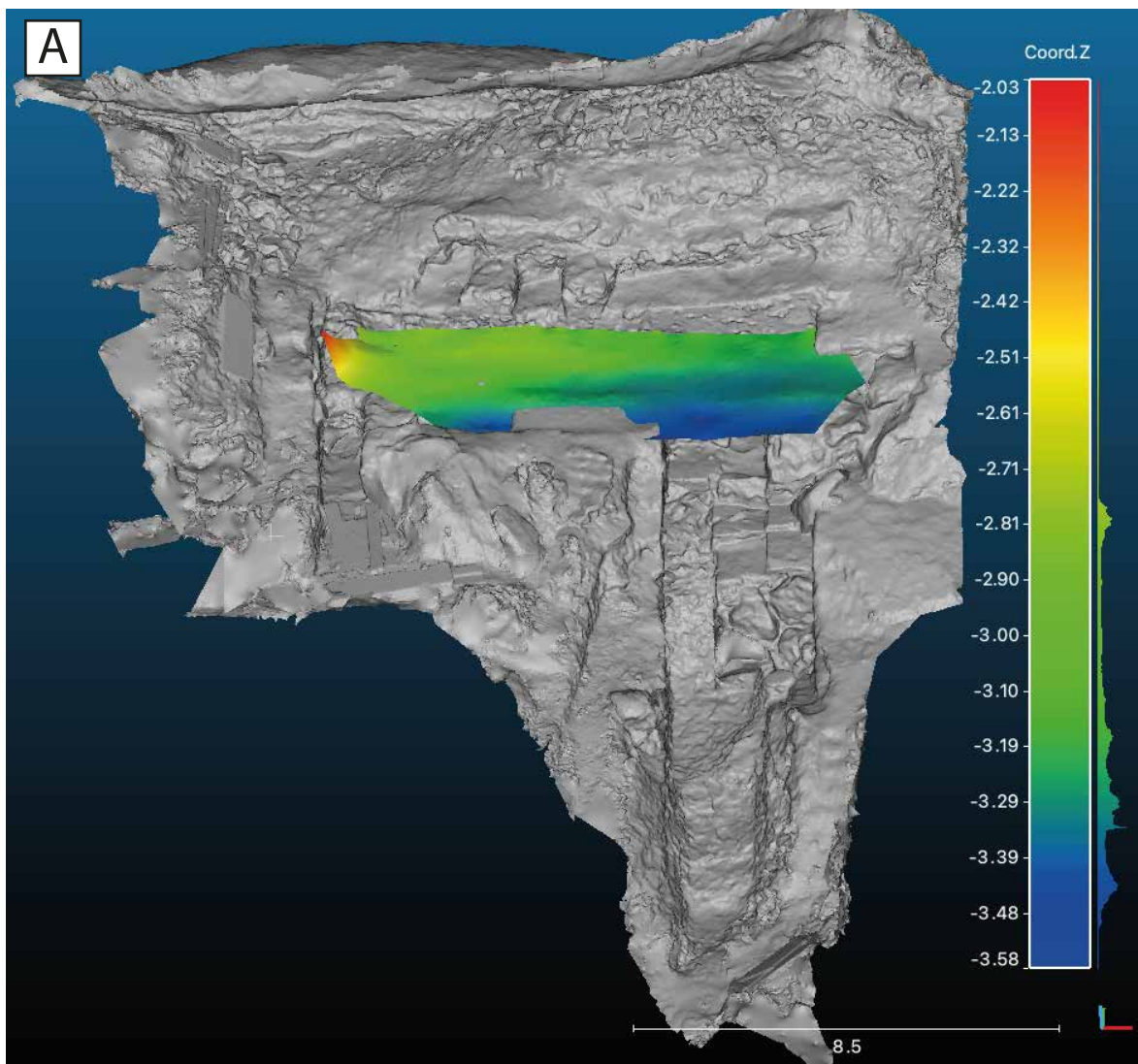


Figure 13

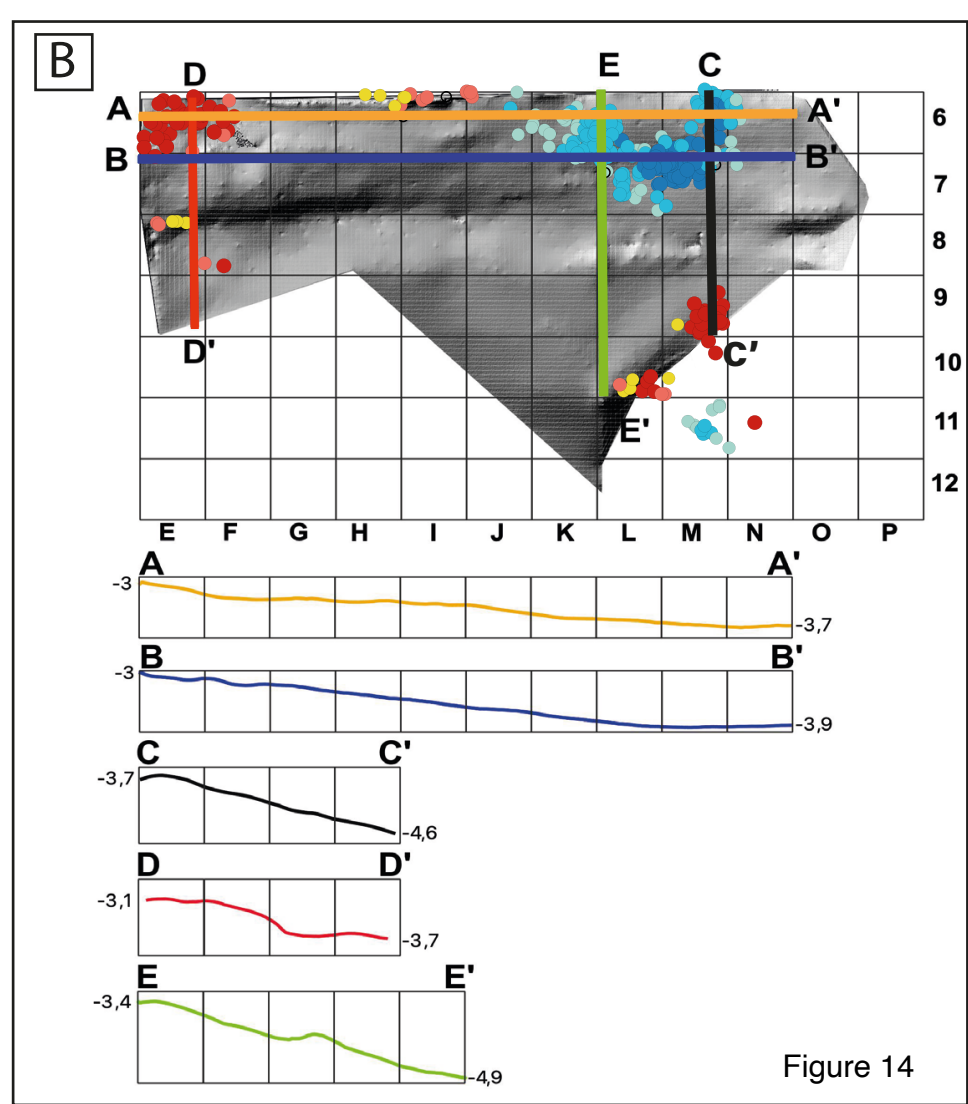
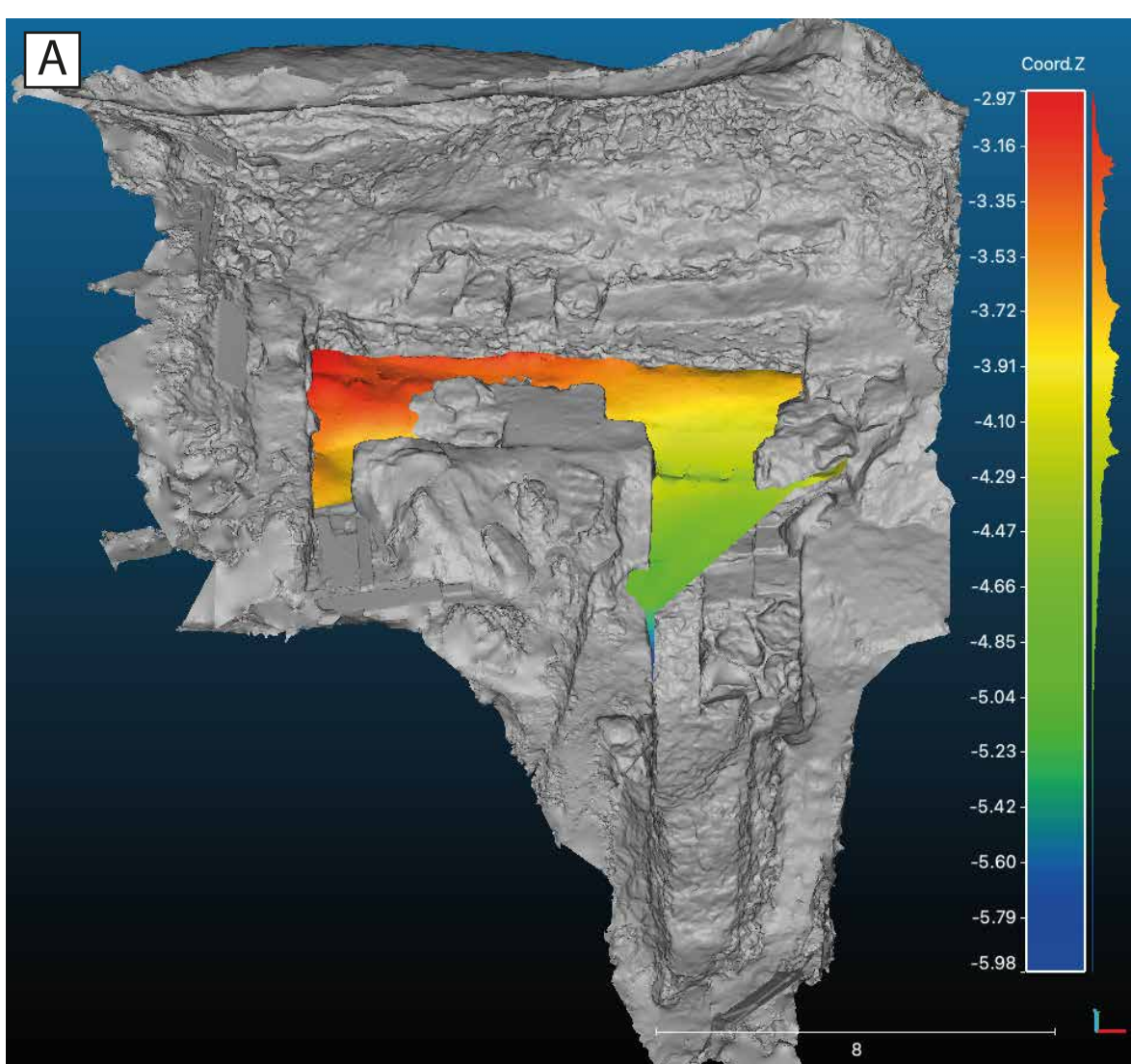
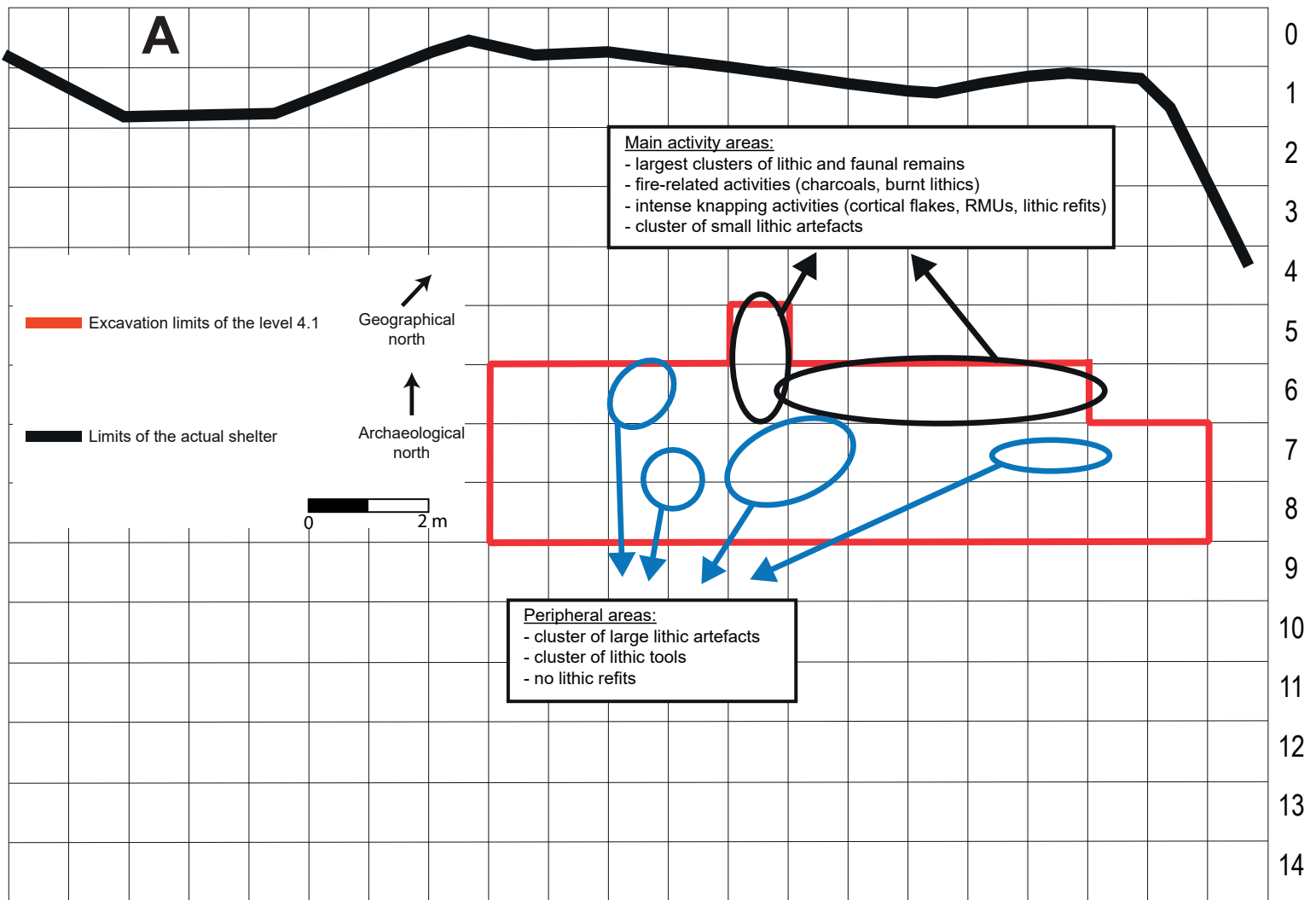


Figure 14



Figure 15

A B C D E F G H I J K L M N O P Q



A B C D E F G H I J K L M N O P Q

